2012-12-14

The Potential of Using Worldview-2 Imagery for Shallow Water Depth Mapping

Alsubaie, Naif Muidh

UNIVERSITY OF CALGARY

The Potential of Using Worldview-2 Imagery for Shallow Water Depth Mapping

By

Naif Muidh Alsubaie

A THESIS

SUBMITTED TO THE FACULTY OF GRADUATE STUDIES

IN PARTIAL FULFILMENT OF THE REQUIREMENTS FOR THE

DEGREE OF DEGREE OF MASTER OF SCIENCE

DEPARTMENT OF GEOMATICS ENGINEERING

CALGARY, ALBERTA

December, 2012

Abstract

Worldview-2 is the first very high resolution satellite imagery that has the ability to acquire data of eight bands named: Coastal (400 - 450 nm), Blue (450-510 nm), Green (510-580 nm), Yellow (585 - 625 nm), Red (630-690 nm), Red Edge (705 - 745 nm), Near Infrared(NIR) 1 (770-895 nm) and Near Infrared(NIR) 2 (860 - 1040 nm). Furthermore, five of these bands — Coastal Blue, yellow, red edge and NIR 2 are the new bands in WorldView-2 that are capable of extracting new features that were not possible with previous satellite imagery. Accurate and up-to-date bathymetric models are an effective tool for gaining a clearer understanding of the world's waterways, and thus play an important role in many marine applications such as navigation. In this research, the automatic feature extraction technique will be used to locate water area edges. A threshold mask will then be used to determine small land and ships inside the shallow water area. An assessment will be done for all the eight bands to show their contribution to the bathymetry application and shore edge and shallow water outlining, with an emphasis on the yellow and Coastal bands. The conclusion and recommendation will be based on a statistical analysis of the comparison between Worldview-2 data and DEM data for the same area of interest.

Acknowledgements

I would like to take this opportunity to express my sincere gratitude and appreciation to my supervisor, Dr. Naser El-Sheimy, who has played significant role in my life. Dr. Naser El-Sheimy opened the door for me to become one of the qualified graduate students of the Geomatics Engineering Department. He never hesitated to answer any of my questions and my requests for guidance never went unanswered. I was very pleased to be under his professional and academic supervision; to him, I owe him my knowledge of Geomatics. Thank you, Dr. Naser for your unwavering support.

I wish to extend my appreciation and thanks to the King Abdullah program for External scholarships—this research would not have been possible without the full sponsorship I have been given from the Saudi Cultural Bureau in Canada, which represents the Ministry of Higher Education in Saudi Arabia.

I would like to extend my gratitude, appreciation and thanks to Dr. Mohamed Elhabiby who stood beside me and helped me develop a deeper remote sensing background. His proposed ideas, valuable discussions and suggestions were important sources information for my research. Also, I would also like to thank him for his time and effort in revising my thesis and published paper.

I wish to extend my thanks to Dr. Sina Taghvakish, who helped me with technical problems, especially with the ENVI program. Also, I would like to thank him for his valuable time and informative discussions.

I would also like to express my thanks to my friends and colleagues in the Mobile Multi-Sensor Research Group: Ahmed Shawky, Mazen Alsadat, Dr. Hassan Elhifnawy, Dr. Sameh Nassar, Dr. Yigiter Yuksel, Dr. Walid ,Adel Moussa, Ahmed El-Ghazouly, Mohamed Attia, Abdelrahman Ali, Bassem Sheta, Sara Saeedi, Xing (Bob) Zhao, Siddharth, Hsiu-Wen Chang , Hussein Sahi, and Amr Al-Hamad. I have had a wonderful time conducting research with all of them. They all made for an excellent work environment.

I would like to thank DigitalGlobe Company and Data Fusion Technical Committees (DFTC), which is part of Geoscience and Remote Sensing Society at IEEE for providing the Worldview-2 data.

Thank you to the Seafloor Mapping Lab at California State University for providing the Sonar data. And last but not least, I would like to thank the U.S. Geological Survey Department for providing the sediment thickness map.

Dedication

To My Beloved Family

My Father & My Mother

My Brother & My Sisters

Table of Contents

List of Tables

List of Figures and Illustrations

List of Symbols, Abbreviations and Nomenclature

Symbol	Definition
WV-2	Worldview-2 Satellite Imagery
GNSS	Global Navigation Satellite System
IMU	Inertial Measurement Unit
SONAR	Sound Navigating and Ranging
LiDAR	Light Detection and Ranging
Δt	The time difference between the transmitted and the received signal
VW	The speed of sound in water
ALB	Airborne LiDAR Bathymetry
ALS	Airborne Laser Scanning
LRF	Laser range finder
SGA	the stratified genetic algorithm
AVIRIS	Airborne Visible Infrared Imaging Spectrometer
BRDF	bi-directional reflectance distribution function
TOA	The top-of-atmosphere
NDVI	The Normalized Difference Vegetation Index
NWDI	The Normal Water Different Index
DEM	Digital Elevation Model
R2	The square of correlation value
B&CB	The ratio between blue and coastal blue bands
B&G	The ratio between blue and green bands
G&CB	The ratio between green and coastal blue bands
R&CB	The ratio between red and coastal blue bands
Y&CB	The ratio between yellow and coastal blue bands
RMS	Root mean square error

Chapter One: **Introduction**

Bathymetry is playing an increasing role in many marine applications, such as marine navigation, oil and gas, and harbours constructions. Although 71 percent of the Earth's surface is covered by water, its oceans, seas, and other water bodies remain poorly mapped. The majority of the world's cities with larger populations are located relatively close to a coast. (Wong et al, 2007) states that of the world's 39 capital cities with populations over 5 million are located within 100 Km of the coast as well as 116 cities with populations greater than 10 million. Bathymetric information therefore becomes an essential tool for such areas as nautical marine navigation, and coastal planning and management. Furthermore, bathymetric data can help improve the study of marine environments, earth sciences, and the effects of human activities have on bodies of water. Militaries and waterways authorities can also benefit from bathymetry since mapping underwater features like rocks, and sand produces accurate depth measurements (HAIBIN et al. 2008). Moreover, bathymetry is an important application for near-shore human activities such as swimming, fishing, and various engineering applications such pipeline, cables, and oil drilling.

Remote sensing imagery has become more common in the study of underwater features and as such is playing an increasingly important role in bathymetric applications. There are two main types of remote sensing: passive and active. The passive technique uses sensors to measure the electromagnetic radiation reflected by the object and produces thermal, multispectral and hyperspectral imagery. In contrast, the active technique requires energy to be emitted so that the reflection produced can subsequently be measured. Lidar, radar and sonar all belong the active sensors family. Mapping shallow coastal waters (shoreline) with echo sounding techniques and hydrographic survey techniques is costly, slow and has certain limitations. Fortunately, remote

sensing offers an alternative solution by evaluating the optical bands' reflectance, which has a high correlation to water depth.

1.1 Motivations

Nowadays, very high resolution multi-spectral satellite imagery, such Worldview-2 (WV 2), can help researchers to study the body of the water bed and to extract shore edges (Globe 2010). WV-2 has the ability to acquire 11-bit data in nine spectral bands: panchromatic, coastal, blue, green, yellow, red, red edge, NIR1, and NIR2. The Coastal Blue band is useful for bathymetric studies because Coastal blue is least absorbed by water. The main motivation of this thesis is to test this satellite mission in general and this band in specific for bathymetric applications.

1.2 Thesis Objectives

The main objective of this research is to assess the use of Worldview-2's new bands for sea bed mapping of shallow water against ground truth and to test the penetration range of different band-ratios. To meet the overall objective of the thesis, the following sub-objectives will be addressed:

1- Evaluate the contribution of the new Coastal blue band for determining water depth.
2- Determine the best band ratios for acquiring the penetration range, especially with the coastal blue band.

1.3 Thesis Outline

The thesis is divided into five chapters. Chapter One provides an introduction and overview of the research objectives and contents.

Chapter Two presents a background of bathymetry and an overview of different techniques that have been used to derive it. These techniques are as follows: echo sounding such as SONAR, LiDAR techniques such as Airborne LiDAR Bathymetry, and satellite imagery techniques. This chapter also introduces an important literature review about deriving and mapping bathymetry from satellite imagery. Finally, the chapter illustrates the features of the new, very high resolution satellite imagery "Worldview-2".

Chapter Three introduces the data used in this research as well as the study area. It explains the methodology including data pre-processing, processing, and evaluation. The chapter will also describe the implementation techniques used for the different band ratio algorithms. Five ratio combinations, through five transects of different locations in the scene, will be introduced.

Chapter Four shows the results of the predicted relative and absolute bathymetry of the above mentioned five transects in addition to the final absolute mean of error for each of the five combination of ratios through each transect.

Chapter Five presents the conclusions of this research and highlights some important suggestions for future work.

Chapter Two: **Background and Literature Review**

2.1 Bathymetry

Bathymetry is the science of measuring the underwater depth of bodies of water (seas, rivers, oceans, etc.). As a result, the topography, such as the seafloor, is determined. The term originates from the Greek words *bathus* meaning "deep" and *metron* meaning "measure". Mapping the seafloor has been known for thousands of years. The safe navigation of ships is one of the primary reasons for mapping the depth of seafloor (Timothy et al. 2010). Currently, there are many techniques for calculating bathymetric measurements such as Sound Navigating and Ranging (SONAR), Airborne LiDAR Bathymetry (ALB), and satellite imagery. The following section includes a brief description of these various techniques in order to clarify the motives for using satellite imagery as a complementary or alternative method.

2.1.1 SONAR

(SONAR) is an important technique for measuring and detecting objects in water. It uses sound to detect the seabed and can be implemented by knowing the speed of the sound in the water column. The acoustic signal is transmitted through the water to the seabed from a transducer located beneath the ship; however, it can also be reflected back and received by the transducer. As a result, the range can easily be calculated by multiplying the time difference (Δt) between the signals being transmitted and received and the speed of sound in water (V_w) as shown in Equation 2.1

$$Range = 1/2 * \Delta t * V_W \quad \textbf{2.1}$$

Certain factors affect the speed of sound in water such as air bubbles, salinity, temperature, and density. These factors should therefore be adjusted and accounted for to prevent any error. Finally, by implementing the Global Navigation Satellite Systems (GNSS) and Inertial Measurement Unit (IMU), the position and attitude of the ship can be determined.

A sonar system has two different types of echo sounders: a single beam sonar, which measures the bathymetry using a single sonar beam and a multi-beam sonar which measures the bathymetry using an array of beams. The single sonar beam produces a strip of measured depths in the direction the ship travels. However, in order to map certain areas, several parallel and overlapped strips must be surveyed. The multi-beam sonar produces a wide swath of measured depths perpendicular to the travel direction, which is produced by a wider strip as shown in Figure 2-1. (McNair 2010)

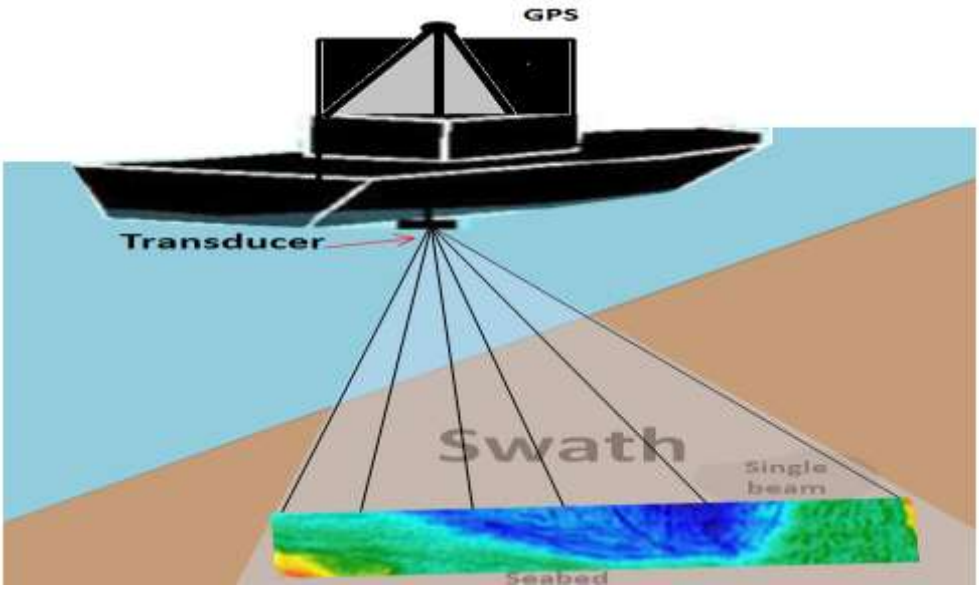

Figure 2-1: Multibeam Echo Sounder.

2.1.2 Airborne LiDAR Bathymetry (ALB)

There are two categories of airborne systems that LiDAR uses: a topographic system to measure terrain heights, such as Airborne Laser Scanning and bathymetric systems to determine water depth, such as Airborne LiDAR Bathymetry. The most significant difference between Airborne Laser Scanning (ALS) and Airborne LiDAR bathymetry (ALB) is the type of laser employed by either technique. ALS uses an infrared laser while ALB uses infrared and green laser (McNair 2010). Airborne LiDAR Bathymetry was designed specifically for determining the depth of shallow water. It is made up of six elements: a Laser Range Finder (LRF), computer, scanner, GNSS receiver, an IMU, and a data storage component (Guenther et al. 2000) .The technique behind ALB is simple— a short pulse, consisting of green and infrared lasers, is transmitted to the water's surface. The green pulse then penetrates the water columns with a maximum attenuation of 70 m, depending on water clarity, and is scattered across the bottom of the water column. The infrared pulse, however, is scattered across the water's surface. Finally, both scattered pulses are measured by a receiver on the aircraft, and the elapsed time between the two pulses is used to determine the depth (Banic et all. 1987). The LiDAR method has the ability to derive accurate bathymetric information for up to 70 m in clear water. However, LiDAR applications are limited given their high cost.(McNair 2010)

2.1.3 Satellite Imagery

Charting by shipboard echo sounding is one of the most traditional methods for deriving bathymetry. It has the ability to produce accurate depth measurements along transects or at points. However, this method has a high operational cost and it cannot be used to derive shallow

water depths. In contrast, bathymetry using remote sensing is more efficient and is significantly more cost effective for mapping remote and broad areas. Remote sensing has two types of methods: an active method such as LiDAR, and passive method such as satellite imagery. As shown in Figure 2-2, satellite imagery is very efficient for mapping large areas and is cost effective. But perhaps what is most significant is that satellite imagery has the ability to derive the water depth of shallow turbid coastal areas (Globe 2010).

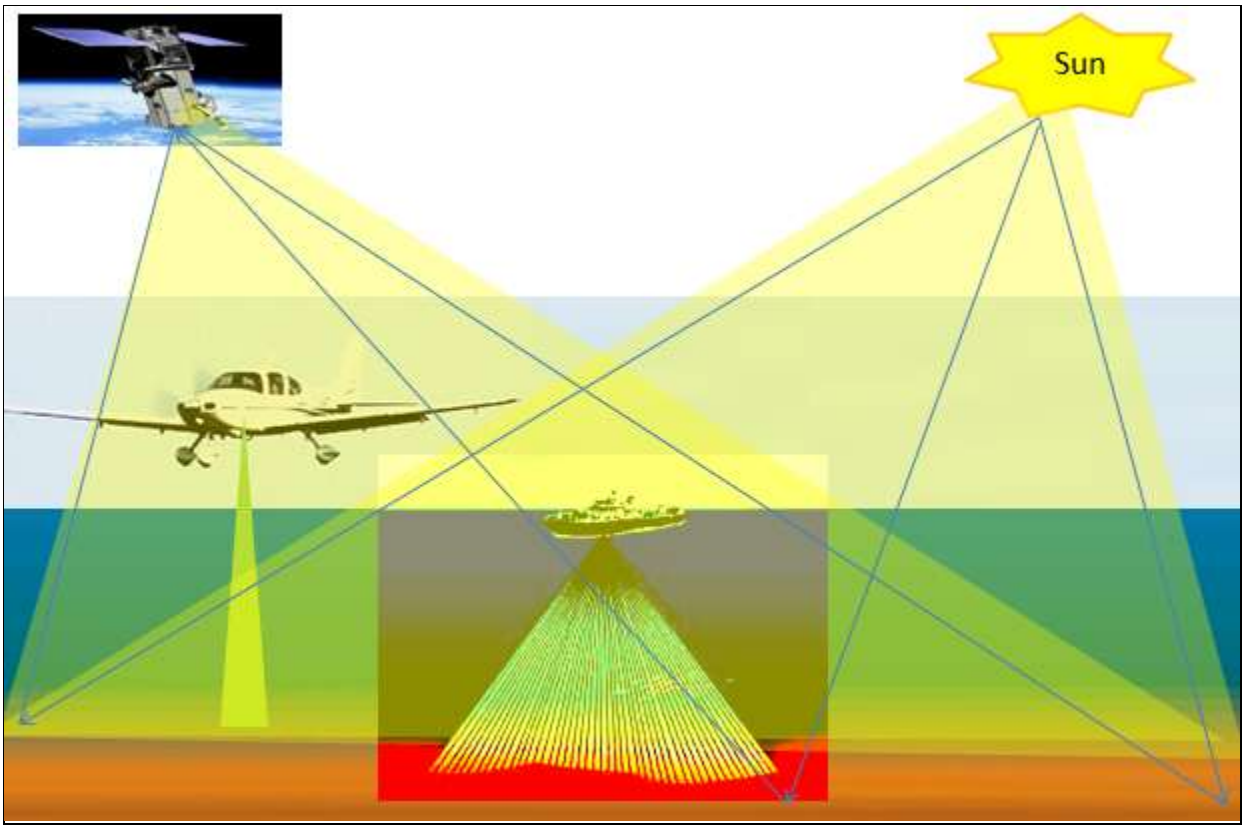

Figure 2-2: The difference between SONAR, LiDAR, and Satellite imagery in term of Large Coverage.

The value of mapping the shallow water environment from satellite imagery has been discussed in several studies, more specifically with the use of visible wavelengths which penetrate greater

water depths (Bierwith et al. 1992), However, with the introduction of the WV-2, the topic is again open to more research and investigation in the assessment of its new bands..

2.1.4 Light Theory

In order to understand how bathymetry is derived from satellite imagery, knowledge of the theory of light transmission is required. Bierwith (1992) states that the basic principle behind deriving water bathymetry is that the radiance received by the satellite is a function of five parameters: incoming solar radiation, attenuation of radiation into and out of the atmosphere, attenuation of radiation into and out of the water column, reflectance properties of the seabed, and the depth of water, shown in Figure 2-3.

The amount of attenuation is based on the wavelength of each band of the satellite imagery. For example shorter visible wavelengths, such as blue, penetrate the water column deeper than a band with longer wavelength such as red, as shown in Figure 2-4.

Given that the WV-2 multiband satellite mission is now equipped with several new bands of shorter wavelengths, the possibility exists for more of bathymetric applications that will be discussed further in this research thesis.

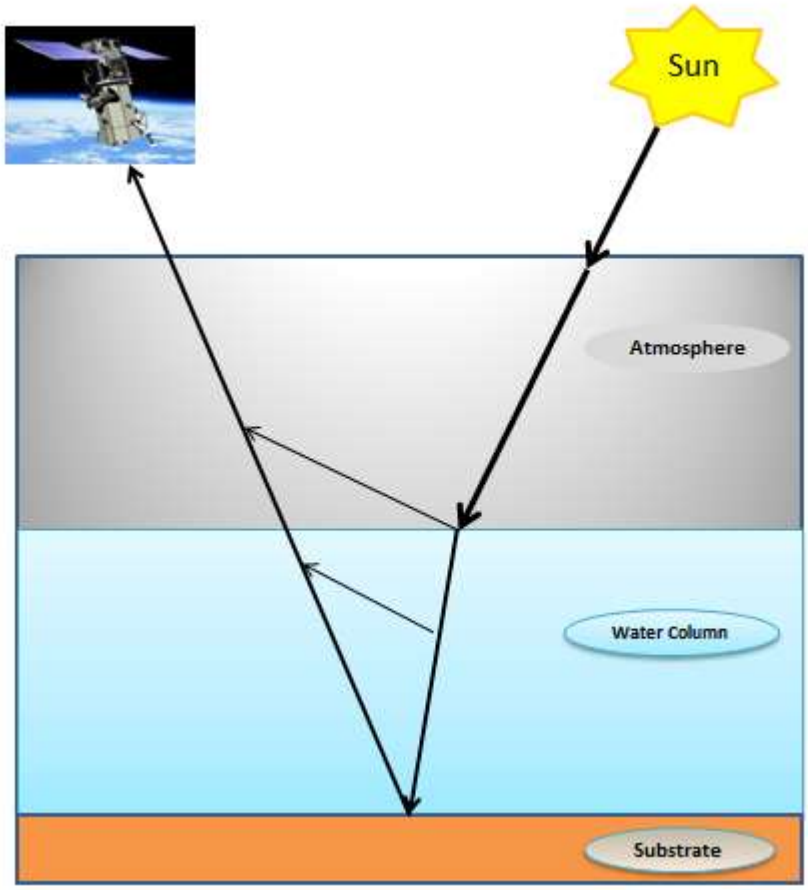

Figure 2-3: Factors that affect the procedure for determining the depth from satellite imagery

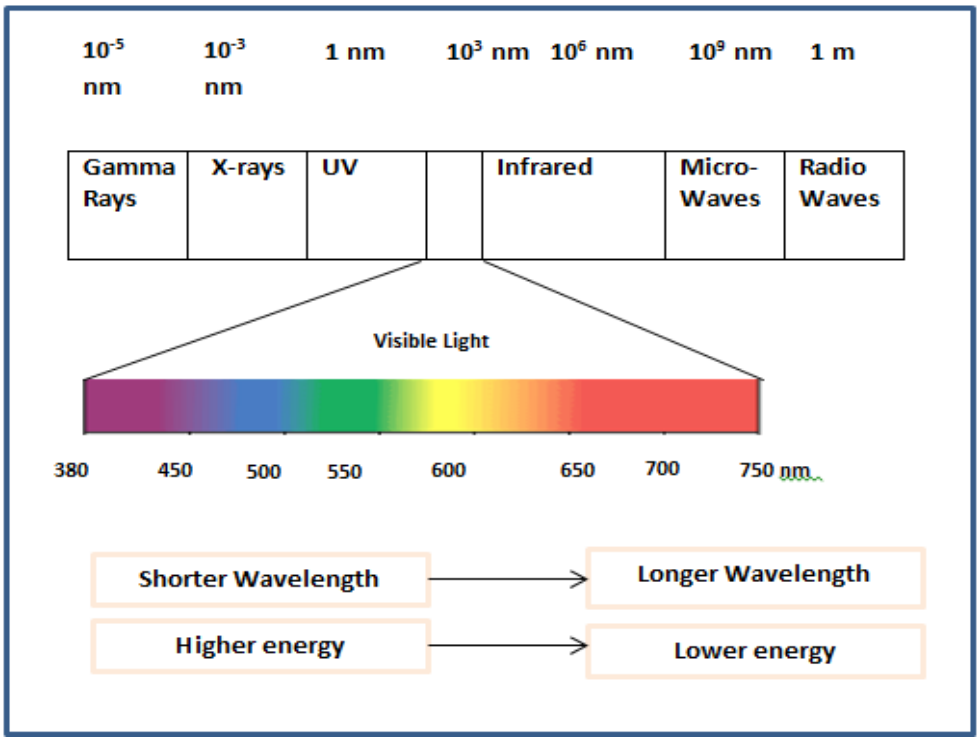

Figure 2-4: Visible Portions of the Electromagnetic Spectrum

2.2 Literature Review

(LYZENGA 1985) devolved a linear technique to determine the water depth. The technique utilized a single band to define the relationship between the reflected radiance and water depth in cases where the optical properties of the water reflectance and the bottom reflectance are constant. This technique was performed under two assumptions. The first assumption was that water properties are homogeneous, meaning the attenuation coefficient is always constant. The second assumption used Beer's Law which states that "light decays exponentially with depth in the water column" which can be expressed by Equation 2.2.

$$R_w = (A_d - R_\infty)e^{-gz} + R_\infty \qquad \textbf{2.2}$$

Where R_w is the reflectance of the water, A_d is the irradiance reflectance of bottom (albedo), R_∞ is the reflectance of the deep water column, z is the depth, and g is the function of the diffused attenuation coefficient for down welling and upwelling light. Therefore, in order to determine the depth equation 2.2 was transferred to Equation 2.3:

$$Z = g^{-1}[\ln(A_d - R_\infty) - \ln(R_w - R_\infty)] \qquad \textbf{2.3}$$

(LYZENGA 1985) also, developed an empirical method referred to the "standard linear transform algorithm" which was used to determine the depth in clear water from passive sensors. This technique is used in cases where the optical properties of the water's reflectance and the bottom reflectance are not constant. This method used one or more of the wavebands to derive the water depth for each pixel as shown in Equations 2.4 and 2.5. However, the algorithm has some limitations such as requiring five tunable parameters and does not work with low albedo water.

$$Z = a_0 + a_i X_i + a_j X_j \qquad \textbf{2.4}$$

Where

The constants $(a_0, a_i, and\ a_j)$ are usually determined from multiple linear regressions. X is the transformed radiance at a specific bands ($_i$, $_j$). R_∞ is the water column reflectance, and R_w is the reflectance of water. In order to have the linearity transform, the natural logarithm was used to linearize the radiance which is expressed in equation 2.5:

$$X_i = \ln[nR_w(\lambda_i) - nR_\infty(\lambda_i)] \qquad \textbf{2.5}$$

(Bierwith et al. 1992) developed a new algorithm that uses a mathematical constraint to avoid mixing the exponential influence of depth in each pixel of the data, as shown in Equation 2.6. This allows some of the multispectral to represent relative substrate reflectance. This study utilized the Landsat TM data in combination with a co-analysis of bathymetry data, particularly the first three bands; blue (450-520, nm), Green (520-600, nm), and red (630-690, nm) which helped achieve a respectable water penetration. Finally, this study allowed for the delineation of seafloor features such as the distributions of sea-grasses, microbial mats, and sandy areas from the color image.

$$Z = \sum_{i=1}^{N} \frac{\ln R_{Ei}}{(-2KiN)} - M \qquad \textbf{2.6}$$

Where, R_{Ei} is the water reflectance, K is the effective attenuation coefficient for the water-body, N is the number of bands used (visible blue, visible green, visible red), and Z is the water depth.

Lyzenga's (1985) method proved inaccurate for calculating water depth since the bottom albedos varied significantly. Therefore, this method contains so much error that it was unable to differentiate between various albedos (Green et al. 2000). As a result of these limitations, (Stumpf et al. 2003) was inspired to develop a new ratio for transforming the reflectance in an attempt to determine the depth utilizing Equation 2.7. Absorption degrees of different bands with different wavelengths were principle behind this method, where each band was attenuating at a different degree while the energy penetrated the water. Therefore, the band with the higher absorption degree decreases consistently faster while the depth increases. As the ratio increases so does the depth increases. To conclude the research work, this method removed the effects of

varying albedo where both bands have a similar effect. The ratio between these bands was affected by the increase in depth more than the varying bottom albedo. As shown in 2.7 this algorithm requires only two tunable parameters which could be computed using the linear regression method between the ratio result and ground truth. The standard linear transform and the ratio transform algorithms were compared using IKONOS satellite imagery as opposed to liDAR bathymetry. In order to compute the ratio algorithm the coefficients (m_1, m_0) were tuned manually to a few depths from a nautical chart. The linear algorithm was tuned using multiple linear regressions against the LiDAR data. (Stumpf et al. 2003) found that both algorithms are equivalent over variable bottom type albedo and retrieve bathymetry in water depths less than 10–15 m. However, while the linear transform does not distinguish depths greater than15 m, ratio transforms can also be applied to low-albedo water. (Stumpf et al. 2003) stated that this method was robust and works well over variable bottom types.

$$Z = m_1 \frac{\ln\left(nR_w(\lambda_i)\right)}{\ln\left(nR_w(\lambda_j)\right)} - m_0 \qquad \textbf{2.7}$$

Where m_1 is a tunable constant to scale the ratio to depth, n is a fixed constant for all areas to assume that the algorithm is positive, and m_0 is the offset for a depth of 0 m where (Z = 0) . R_w is the reflectance of water, and (λ_i, λ_j) are two different bands.

(Densham 2005) used multi-spectral QuickBird imagery to derive seabed bathymetry at two separate locations (Looe Key, USA and Plymouth Sound, UK) with different water conditions and clarity. Their study employed two methods, the ratio method and the stratified genetic algorithm (SGA). The SGA algorithm divides the water column into levels of differing

attenuations (based on turbidity) and calculates the sum of ratios for several wavelengths (Gianinetto et al, 2003). Both methods were used to determine the bathymetry for each area. Bathymetric data from LIDAR and charts were compared to the QuickBird data in order to derive the depths and evaluate their accuracies. The results showed that each method was influenced by the variable bottom types, light attenuation, surface waves, and non-homogenous water. However, the first method provided a higher accuracy than the second. Densham (2005) concluded that a variable bottom type should be analyzed individually to potentially improve the depth outputs. This study also demonstrated the benefits of a green and red band ratio in more turbid waters.

(Camacho 2006) evaluated the contribution of variable benthic substrates the ratio algorithm's accuracy using multi-spectral QuickBird imagery at Midway Atoll. The QuickBird imagery was classified into two main bottom types while the coefficients were tuned separately for each substrate. Bathymetry was subsequently determined in two stages where the first derived the bathymetry over the separate bottom types of the scene, and the second determined the depth over the whole scene. The results produced from these two stages were then compared. (Camacho, 2006) found that the performance of this model helped improve the accuracy of bathymetric derivation in remote coastal areas. This study highlights the fact that the ratio algorithm does not compensate for variable bottom type and albedo.

(Loomis 2009) studied the effect of using additional yellow spectral band in combination with blue and green bands in order to derive bathymetry. Worldview-2 was not yet launched at the time of this study. Therefore, a hyper-spectral image acquired from the AVIRIS (Airborne Visible Infrared Imaging Spectrometer) sensor was used as a temporary image for the Worldview-2 multispectral sensor. The image was processed using the (Stumpf et al. 2003)

"ratio method" to determine bathymetry. The results showed that when the yellow/green and yellow/blue ratios were incorporated into the algorithm, the accuracy of bathymetric measurements was greater than when the green/blue ratio was used, particularly in shallow waters.

(D.Parthish et al. 2011) used Worldview-2 data to estimate relative bathymetry with notable corrections to determine ocean depth. Relative bathymetries using the coastal blue and blue bands were derived from NIR2 with a linear regression analysis for the atmosphere and de-glinting corrections. The results indicated a good regression for the coastal blue band over the shallow coastal.

(McCarthy 2010) used wave motion to observe a rapid succession of multiple images from Worldview-2 satellite imagery of Camp Pendleton, California. The same wave in these multiple images was compared with the exact time at which the image was captured. As shown in Equation 2.8, the linear finite dispersion relation for surface gravity waves was performed to determine the near-shore bathymetry. The wave position and the measured wavelengths were enhanced using image processing techniques. Then, the accuracy of the estimated depth was calculated by comparing the estimated bathymetry to reference bathymetric data. This study was successfully able to determine the water depth with an error of ±15 %.

$$C^2 = \frac{g}{k} tanh(kh) \qquad \textbf{2.8}$$

Where C is the wave celerity, g is the gravitational acceleration constant, k is the wave number $(k = \frac{2\pi}{\lambda})$, and h is the water depth.

(Madden 2011) used data that was captured by Worldview-2 to support the main research objective which was to show that the ratio algorithm that combines the yellow band with the blue, green and red bands can be used separately to derive the relative bathymetry as shown in Equation 2.9. These three ratio results were compared to the blue/green ratio and a green/red ratio in order to evaluate the contribution of the yellow band. Three transect lines were drawn in a shallow reef area to derive the absolute bathymetry. The results showed that the contribution of the yellow band provided more information about the bathymetry than the previous blue/green and green/red combinations. However, the yellow band showed less sensitivity to the variations in bottom type. Therefore, this band was used in this research as one of the ratios combinations beside the coastal blue band. Madden (2011) concluded that the use of this band should be included in the combinations of ratios, but further testing was not conducted.

$$Z = m_1 \frac{\ln\left(nR_w(\lambda_i)\right)}{\ln\left(nR_w(\lambda_j)\right)} - m_0 \qquad \textbf{2.9}$$

Where Z is the depth, m_1 is a calibration coefficient, $R_w(\lambda)$ is the water leaving reflectance per wavelength, n is a constant to keep the ratio positive and m_0 is a correction term for zero depth. The (Stumpf et al. 2003), ratio is a valuable method to use for an area where traditional surveying methods fail to produce adequate information.

Digital Globe Company, which stands behind Worldview-2, states that the coastal blue detector (400-450nm) "supports bathymetric studies with unsurpassed accuracy" (Globe 2010). The ratio produced when the yellow band is combined with the coastal blue band allows for a calculable water depth. Since the coastal blue band has not been previously used in other studies this research will evaluate the contribution of the new band while employing the (Stumpf et al.

2003) ratio algorithm. The coastal blue band will be used in various combinations with other visible bands such as blue, green, red, and yellow in comparison with (Stumpf et al. 2003) ratio, which used blue and green bands.

2.3 Worldview-2 (WV-2) Satellite Imagery

Worldview-2 is new very high-resolution commercial satellite. It was launched from the Vandenberg Air Force Base in October 2009 by Digital Globe, a company that operates two other satellites presently in orbit—WorldView-1 was launched in 2007, and QuickBird was launched in 2001. WV-2, which began operations on January 4, 2010, has an estimated mission life of 7.25 years. It operates at an altitude of 770 kilometers, and has an average re-visit time of 1.1 days where it can collect up to 785,000 square kilometers of eight multispectral bands imagery per day. It is also capable of collecting panchromatic imagery with 0.5 m resolution, eight-band multispectral imagery with 1.8 m resolution and has a nominal swath width of 16.4 kilometers. In addition, WV-2 can acquire 11-bit data in nine spectral bands including panchromatic, coastal blue, blue, green, yellow, red, red edge, NIR1, and NIR2.WV-2 uses a push-broom mechanism to build an image one row at a time as the focused image from the telescope moves across the linear detector arrays. Red-Edge sensor is a new technique that makes WV-2 more powerful than other, older satellites. Red-Edge sensor is part of the 8-band multispectral capabilities and can detect a narrow band of radiation from 705 to 745 nm. This enables the sensor to measure the Red-Edge reflectance with 1.84 m spatial resolution. This combination of spatial and spectral resolution helps segment physical features and provides some measurement of plant vitality.(Globe 2010).

2.3.1 The Properties of the 8 Spectral Bands:

In this section all eight bands will be described and the benefits of each band will be illustrated separately as well as the contribution of each band to this research thesis.

2.3.1.1 Coastal Blue band

This band covers a spectral range between 400 nm and 450 nm as shown in Figure 2-5. This band is one of the new bands which Worldview-2 provides for the remote sensing field. Because it is absorbed by chlorophyll it helps to detect healthy plants and has a useful role in performing vegetation analysis procedures. Since coastal blue is least absorbed by water, it is highly beneficial for bathymetric studies. Therefore, this band is used in combination with different band ratios such as blue, green, red, and yellow, to evaluate its contribution in determining the water depth utilizing equation 3.7.

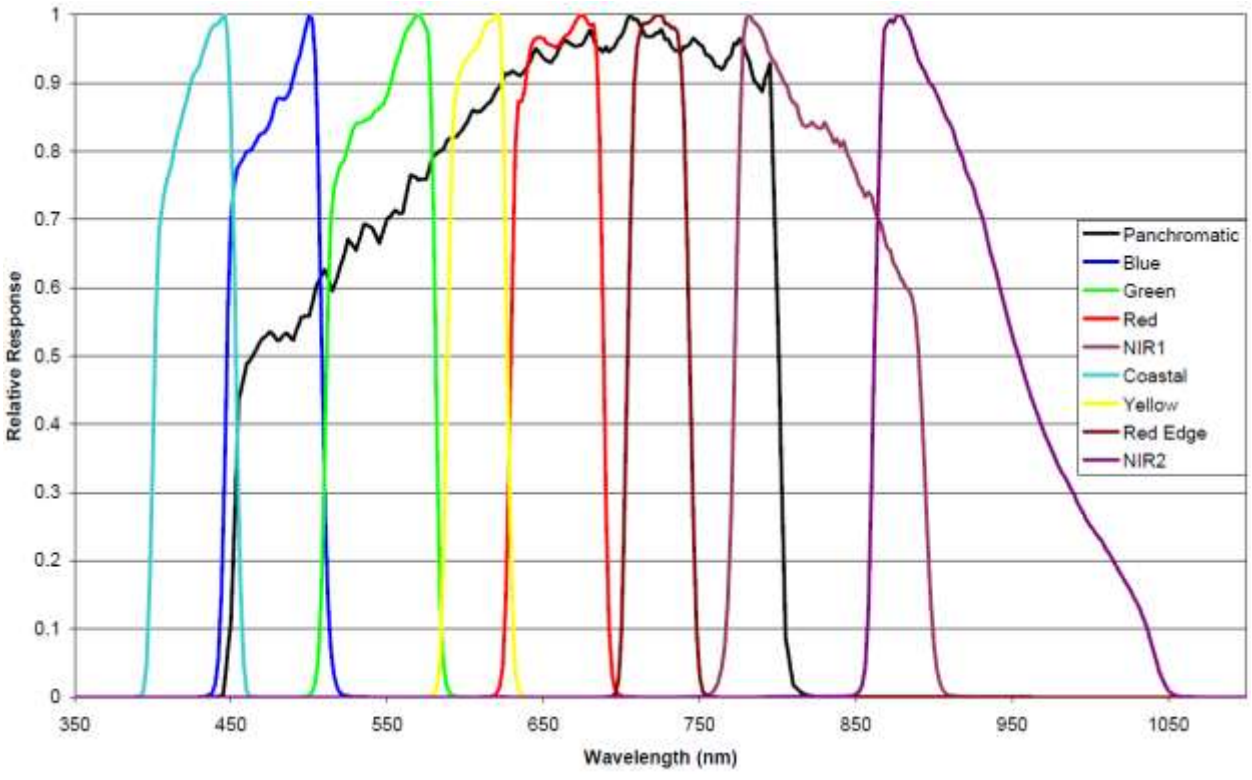

Figure 2-5: Spectral Bands of Digital Globe's Worldview-2 Satellites (Globe 2010)

2.3.1.2 Blue Band

The blue band has spectral range between 450 nm and 510 nm. This is equivalent to Quickbird's blue band, is also absorbed by chlorophyll in plants and delivers good penetration of water. However, when comparing the blue band to the coastal blue band, the latter is less affected by atmospheric scattering and absorption (Lee et al. 2011). This band was used as one of the combinations of band ratios with the coastal blue band to derive the relative bathymetry using equation 3.7

2.3.1.3 Green Band

This band is narrower than the green band on QuickBird and covers a spectral range between 510 nm and 580 nm. It helps detect healthy vegetation by focusing more precisely on the peak reflectance. It remains the best choice for calculating plant vigor and, when combined with the yellow band it becomes very useful for distinguishing different types of plant material (Globe 2010). This band was used as one of the combinations of band ratios with the coastal blue band to derive the relative bathymetry using equation 3.7.

2.3.1.4 Yellow Band

The yellow band covers a spectral range from 585 nm to 625 nm. Also, new to the remote sensing field, this band is capable of detecting the "yellowness" of certain vegetation on land and in water and can be very helpful for feature classification (Globe 2010). This band was used as one of the combinations of band ratios with the coastal blue band to derive the relative bathymetry using equation3.7.

2.3.1.5 Red Band

Narrower than the red band on QuickBird, this band holds longer wavelengths as it covers a spectral range from 630 nm to 690 nm. It is an important band for vegetation discrimination and plays a significant role in classifying bare soils, roads, and geological features. The red band has a better focus on the absorption of red light by chlorophyll in healthy plant materials (Globe 2010). This band was used as one of the combinations of band ratios with the blue band to derive the relative bathymetry using equation 3.7.

2.3.1.6 Red-Edge Band

This is a new band in the remote sensing field. It is useful for detecting vegetation response since it is centered at the onset of the high reflectivity portion between a spectral range of 705 nm and 745 nm. It is useful for classifying vegetation and measuring plant health (Marchisio et al. 2010).

2.3.1.7 Near Infrared One (NIR-1) Band

This band offers greater separation between it and the Red-Edge sensor, which makes it narrower than the NIR1 band on QuickBird. It covers a spectral range between 770 nm to 895 nm and is useful for estimating moisture content and plant biomass. It can effectively distinguish soil types, categorize vegetation types, and separate bodies of water from vegetation (Globe 2010).

2.3.1.8 Near Infrared Two (NIR-2) Band

NIR2 covers a spectral range between 860 nm to 1040 nm. There is overlap between NIR2 and NIR1; NIR2 is a new band for the remote sensing field introduced in WV-2. It is less affected by

atmospheric influence and has the ability for broader biomass studies and vegetation analysis (Globe 2010). When combined with a green band this band is used to perform the Normalized Water Different Index for extracting (NWDI) the water body. According to (Madden 2011), the radiance value of the new NIR2 band is higher over land than over water.

Chapter Three: **Data Used and Methodologies**

3.1 Data Used and Study Area

There are three different data that have been used that covers the same study area in this research. The first data was captured by Worldview-2 very high special resolution imagery in eight spectral bands as shown in Figure 3.1. These multispectral bands are in spectral rang of 400 nm to 1050 nm. The second data was collected with multi-beam sonar with a 1 meter grid value as shown in Figure 3-2. The last data was Sediment thickness map, calculated by U.S Geological Survey from acoustic profiles acquired in the 1960s and from multi-beam bathymetry in 1997 as shown in Figure 3-3.

3.1.1 Worldview-2 Imagery Data

The west bay region of the San Francisco Bay is the study area for this research work. This location was chosen because of the availability of the three sets of data mentioned above. The availability of ground truth data for the same location was provided by the Seafloor Mapping Lab at California State University. The Worldview-2 data was taken on 09 October 2011 with clouded cover equalling zero and with North West Lat = 37.81683659 North West Long = -122.52875537; South East Lat = 37.68933632; South East Long = -122.34765625as shown in Figure 3-1. This data was provided by Data Fusion Technical Committees (DFTC), which is part of Geoscience and Remote Sensing Society at IEEE.

Figure 3.1: Worldview-2 Imagery(DFTC 2012) **Figure 3-1: Study Area Imagery**

3.1.2 Multi-beam SONAR Data

The DEM ground truth data was provided by California State University, Seafloor Mapping Lab and was collected using multi-beam sonar with a 1 meter grid value. This data was plotted using ArcMap software in order to compare it with Worldview-2 data as well as to illustrate different water depths in the overlapped area as shown in Figure 3-2.

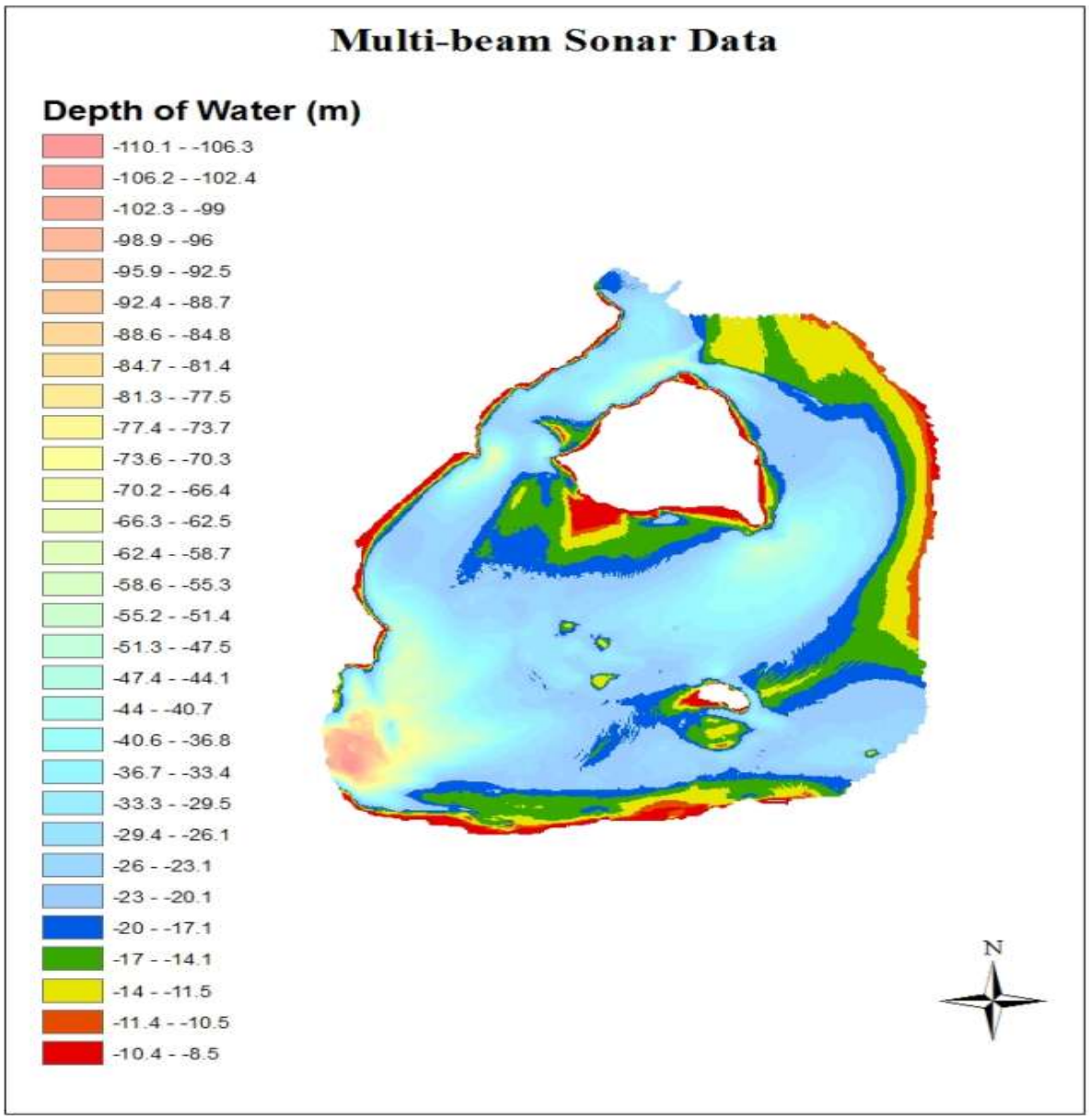

Figure 3-2: Multi-Beam Sonar Data

3.1.3 Sediment Thickness Map Data

This map was the only available sediment thickness map for the study area. It was calculated by the U.S Geological Survey from acoustic profiles acquired in the 1960s and from multi-beam bathymetry in 1997 as shown in Figure 2-4. Although, this is an old data set, it was very useful in the assessment of WorldView-2's new bands. The nature of this area shows no significant change in sedimentation properties since this time.

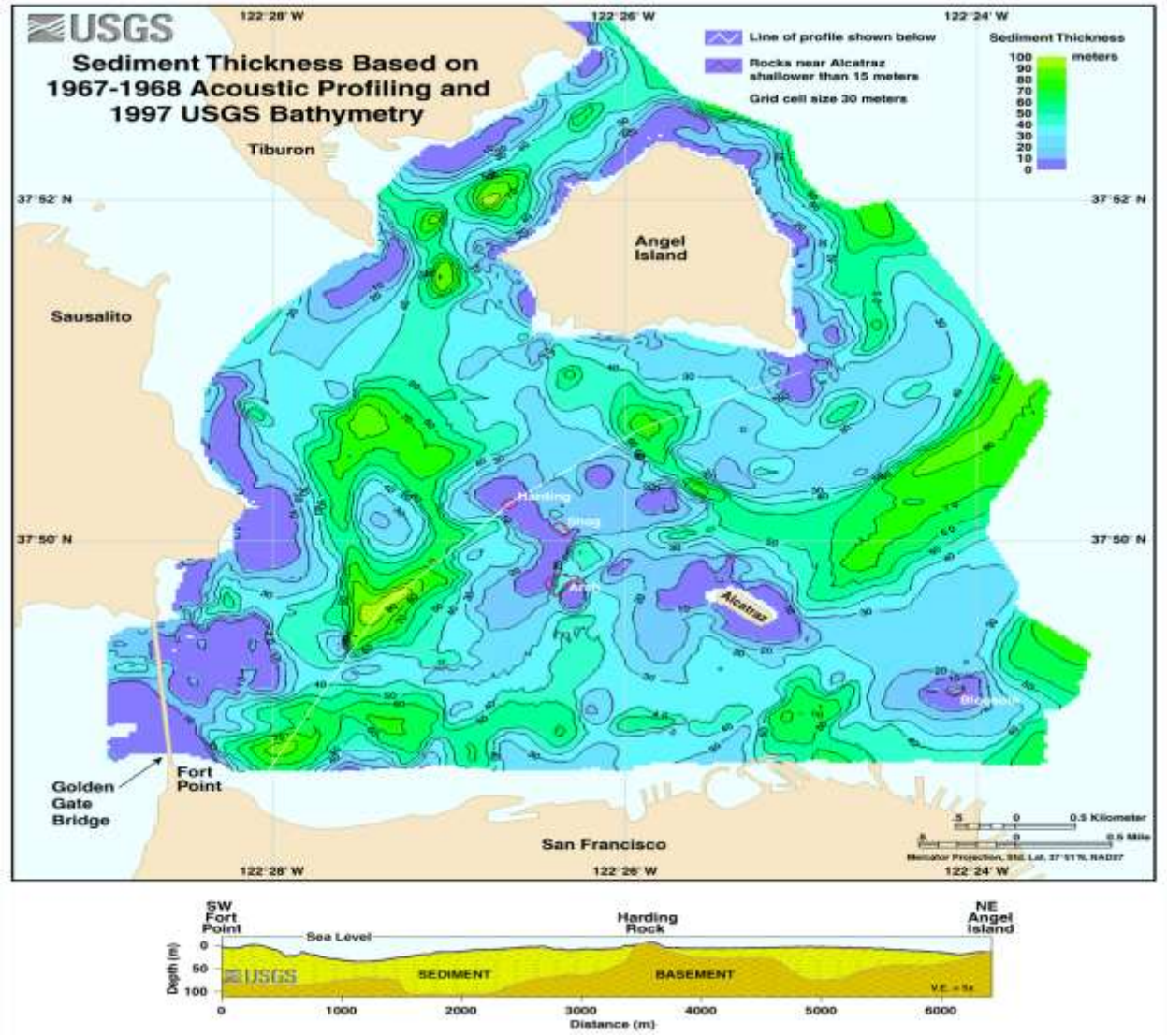

Figure 3-3: West-Central San Francisco Bay Sediment Thickness Map

3.2 Methodologies

The purpose of this research thesis is to derive bathymetry using the Worldview-2's new coastal blue band in combination with the other four visible bands through the Ratio transform method. The goal is to evaluate the contribution of the coastal blue band when added to other bands utilizing the (Stumpf et al. 2003) algorithm as will be shown in Equation 3.8. The results will then be compared to the combination of bands they used, which was the blue and green bands ratio. Figure 3-4 shows the steps involved in deriving bathymetry from Worldview-2 data in four phases. The first phase contains five main steps to perform spectral corrections to the data. The second phase consists of three steps for extracting the water bodies and eliminating non-water classes as well as enhancing the data. The third phase is the process of determining the final bathymetry product from Worldview-2. The last phase is the evaluation of the predicted bathymetry from Worldview-2 Satellite Imagery.

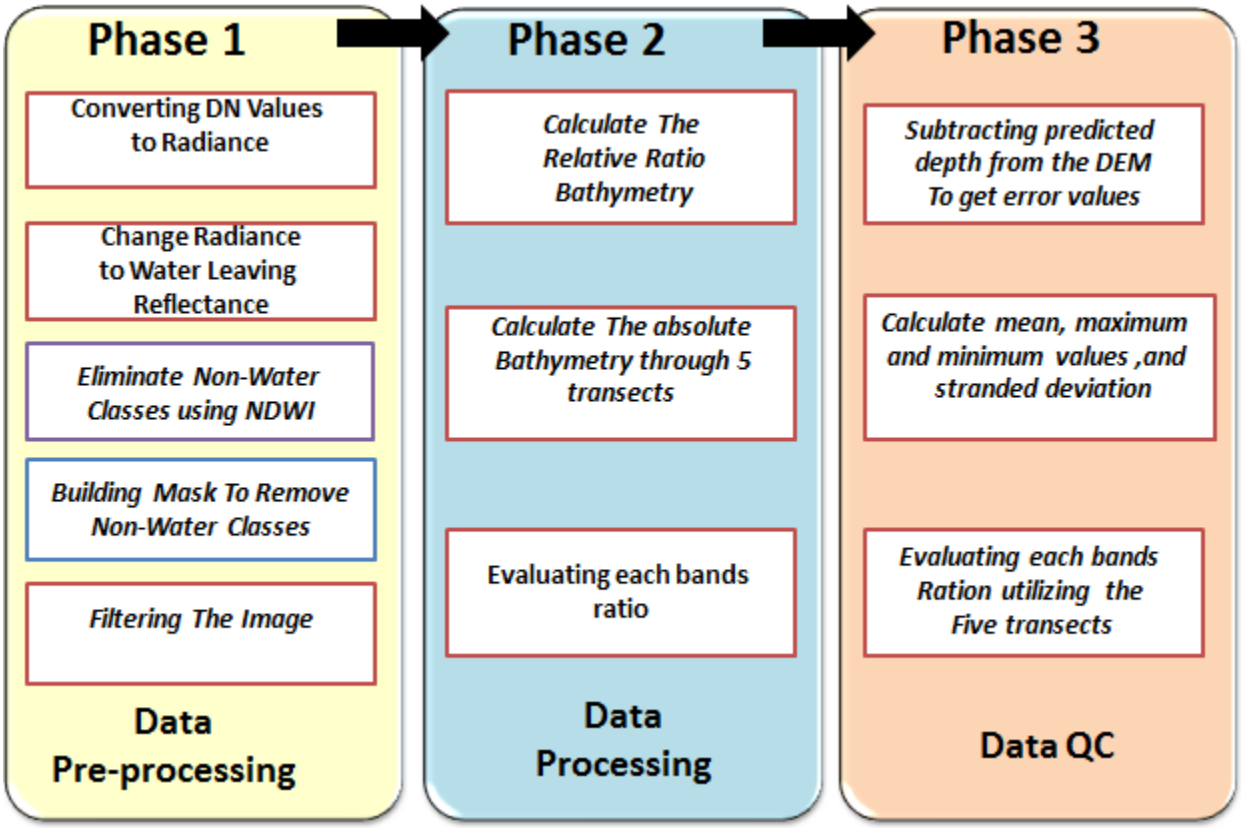

Figure 3-4: The Methodologies Chart

3.3 Data Pre-processing

DigitalGlobe provides customers with Worldview-2 data that are radiometrically corrected image pixels. These image pixels are unique to Worldview-2 data, which are impossible to compare to imagery data from other sensors, especially from a radiometric/spectral point of view. Therefore, the image pixels must be converted to top-of-atmosphere spectral radiance. This research employs an algorithm referred to as the "Ratio transform of reflectance algorithm". This ratio algorithm is based on the reflectance of two bands. Therefore, the DN value must be converted to radiance value in order to change the radiance to the reflectance. Once this occurs, the algorithm can be directly implemented. However, top-of-atmosphere spectral radiance is affected by many factors such as earth-sun distance, topography, solar zenith angle, and bi-directional reflectance

distribution function. To account for these factors, the top-of-atmosphere spectral radiance should be converted to reflectance, which is useful when performing spectral analysis techniques, such as transformations, band ratios, and the Normalized Difference Vegetation Index (NDVI), etc. (Elsharkawy et al. 2012).

3.3.1 Convert the satellite digital numbers to radiance

DigitalGlobe provides raw multi-spectral satellite data in the form of digital numbers (DN). These DN values were converted to top-of-atmosphere (TOA) spectral radiance, which is defined as the spectral radiance entering the telescope aperture of Worldview-2 (Updike and Comp 2010). This procedure was executed using Equation 3.1:

$$L_{\lambda pixel,Band} = \frac{K_{Band}.q_{pixel,Band}}{\Delta\lambda_{Band}} \quad \textbf{3.1}$$

Where $L_{\lambda pixel,Band}$ are TOA spectral radiance image pixels $[\mathrm{W.m^{-2}.sr^{-1}}.\mu\mathrm{m^{-1}}]$, K_{Band} is the absolute radiometric calibration factor for a given band, $q_{pixel,Band}$ is a DN values and $\Delta\lambda_{Band}$ is the effective bandwidth in μm for a given band. Moreover, the calibration factor for each band and the effective bandwidth is included in the image metadata file (IMD) which provides the multi-spectral data. Table 3-1 summarizes both of these quantities for each of Worldview-2's eight multispectral bands.

Table 3-1: Absolute Radiometric Calibration and Effective Bandwidth for the Given Bands

Spectral Band	K_{Band} (W.m-2.sr-1.count-1)	$\Delta\lambda_{Band}$ (μm)
Coastal Blue	9.30E-03	4.73E-02
Blue	1.78E-02	5.43E-02
Green	9.71E-03	6.30E-02
Yellow	5.101E-03	3.74E-02
Red	1.10E-02	5.74E-02
Red Edge	4.54E-03	3.93E-02
NIR1	1.22E-02	9.89E-02
NIR2	9.04E-03	9.96E-02

3.3.2 Change Radiance to Water Leaving Reflectance

The last step in the DN value is to convert the top-of-atmosphere (TOA) spectral radiance. However, this TOA spectral radiance is subjected to four factors: earth-sun distance, topography, solar zenith angle, and bi-directional reflectance distribution function (BRDF). Therefore, the TOA spectral radiance should be converted to reflectance using Equation 3.2. This procedure enables conducting spectral analysis techniques such as band ratios, etc. (Updike and Comp 2010).

$$\rho_{\lambda pixel,Band} = \frac{L_{\lambda pixel,Band}.d_{ES}{}^{2}.\pi}{Esun_{\lambda Band}\ COS(\theta_s)} \qquad \textbf{3.2}$$

Where $\rho_{\lambda pixel,Band}$ is the band-averaged reflectance, $d_{ES}^{\ 2}$ is the distance between the earth and the sun at the time of collection, $Esun_{\lambda Band}$ is the solar irradiance and θ_s is the solar zenith angle. The information found on the IMD file about the satellite and solar geometry at the time of the collection was used to calculate the water leaving reflectance.

As shown in Equation 3.3, and Equation 3.4, the distance between the sun and the earth is in astronomical units as well as the day of the year (Julian date) and the solar zenith angle(Updike and Comp 2010):

$$JD = int[365.25(year + 4716)] + int[30.6001(month + 1)] + day + \frac{UT}{24.0} + B - 1524.5 \quad \textbf{3.3}$$

$$d_{ES} = 1.00014 - 0.01671.cos(g) - 0.00014.cos(2g) \quad \textbf{3.4}$$

The solar irradiance values for all eight bands were made available by the data provider as shown in Table 3-2.The value of the earth-sun distance for Worldview-2 should be between 0.983 and 1.017. This value was calculated using Equation 3.4 based on the following information:

- The WV-2 was launched on October 9, 2011 at 19:36:30 GMT which corresponds to the Julian Day 2455844, which was available on the metadata.
- The earth-sun distance was 0.996606 AU.
- The average solar zenith angle was calculated for the whole image at the time of acquisition using Equation 3.5.

$$\theta_s = 90.0 - sunEl \quad \textbf{3.5}$$

Table 3-2: WorldView-2 Band-Averaged Solar Spectral Irradiance

(Updike and Comp 2010)

Spectral Band	Esun $_{\lambda Band}$ **[W-m-2-μm-1]**
Coastal	1758.2229
Blue	1974.2416
Green	1856.4104
Yellow	1738.4791
Red	1559.4555
Red Edge	1342.0695
NIR1	1069.7302
NIR2	861.2866

3.3.3 Eliminating non-water classes

In order to derive the bathymetry (depth of water) the water body must be extracted from other classes by eliminating non-water classes as well as the shoreline shape by using The Normal Water Different Index (NWDI). This was performed through Equation 3.6. (McFEETERS 1996).

$$NWDI = \frac{(Green - NIR2)}{(Green + NIR2)} \qquad \textbf{3.6}$$

Where the green band is reflected light and NIR2 is reflected near-infrared radiation which had a higher radiance value over land than water. Thus, the NWDI uses NIR2 wavelength to minimize the reflectance off a water feature, while green light wavelength maximizes the reflectance of water features in comparison to land features (McFEETERS 1996). Therefore, the use of NWDI is useful for giving the water feature positive values and the soil and terrestrial vegetation negative values as shown in Figure 3-5. Moreover, this ratio algorithm could have value between -1 and 1, where the positive value is most likely water.

Figure 3-5: NWDI= (Green-NIR2)/ (Green+NIR2)

3.3.4 Masking Land and Non-Water Features

A mask is a binary image that consists of values of 0 and 1.The primary use of masking is to isolate an area of interest, which is used to perform the processing steps. Therefore, this area can be easily differentiated from the rest of the image (Gonzalez and Woods 2002). The threshold for the mask was based on visual observation in order to maximize the coverage of the water body

while minimizing the un-wanted pixels, such as land and non-water features .The NWDI result was used to build mask, where the minimum value of the water class was calculated based on a maximum likelihood estimation technique. Therefore, the minimum value of the water class was chosen as 0.57 based on reference points as shown in Figure 3-6.

Figure 3-6: The Mask

3.3.5 Filtering the image

The median filter is one of the most important filters for removing noise in an image. The function of median filter is to decide if the pixel is or is not representative of the neighboring pixel. Thus, it organizes the pixels in a window that contains the neighborhood from lowest to highest and selects the median value for these pixels which are then replaced in the central of the window (Jensen 1995). The mask mentioned in the previous section was able to remove the noise in a water class that is below 0.57; however, there was some residual pixels left in the image, such as boats and boats wakes. Therefore, the median filter was used on a (7*7) window to remove these unwanted pixels as shown in Figure 3-7. The unwanted pixels from ships and

their wakes were in the order of 4 pixels and therefore, in a (7*7) window they were a minority, which could be removed by the median filter.

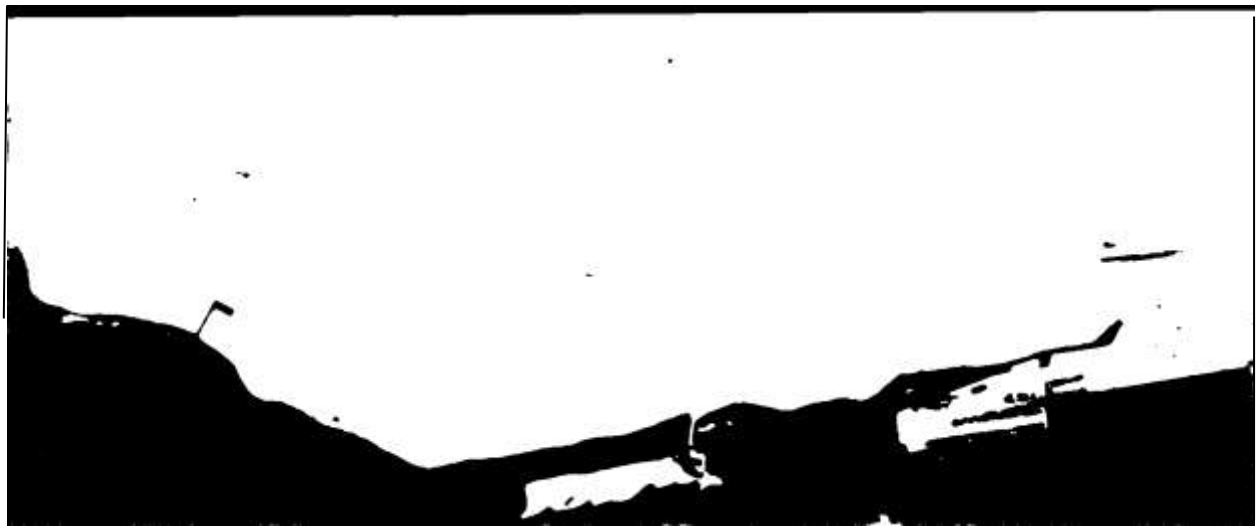

Figure 3-7: Median Filter

3.4 Data processing

3.4.1 Calculate the relative ratio bathymetry

Equation 3.7 was used to create different combinations of relative ratio (relative ratio depth) between spectral bands. The first is the blue/green ratio which (Stumpf et al. 2003) used for their algorithm. The last three ratios are combinations with the new coastal blue band and occur as follows: blue/coastal blue, green/coastal blue, red/coastal blue, and yellow/ coastal blue by using equation3.7. In each case the shorter water leaving reflectance wavelength Rw(λi) is in the numerator and the longer wavelength Rw (λj) is in the denominator (Alsubaie et al. 2012).

$$Z = \frac{1n\left(nR_w(\lambda_i)\right)}{1n\left(nR_w(\lambda_j)\right)} \quad \textbf{3.7}$$

Where n is a fixed constant for all areas in order to keep all values positive. R_w is the reflectance of water, and (λ_i,λ_j) are two different bands.

3.4.1.1 Validation of Worldview-2 for Bathymetry against DEM

The ability of each band ratio combination, mentioned above, to derive bathymetry will be evaluated. The predicted absolute bathymetry will also be calculated. Therefore, some corresponding points between the ground truth (DEM) and each relative ratio must be selected. Hence, five transects with different locations and a different number of pixels were selected as shown in Figure 3-8 and Table 3-3. The locations of each transect was chosen based on the visual observation of each area from where each one was selected. For instance, it is immediately noticeable where transect one is located since there is a sudden change in the water. The first, second, third, and fifth transects were perpendicular to the shoreline in order to be with the water movement, however, transect four was selected with angle of 45^0 in order to be against the water movement.

Figure 3-8 : Transects' Locations

Table 3-3 shows the distributions of the five transects as well as lists the number of pixels, locations, and number of referenced (corresponding) points for each transect.

Table 3-3**: Transects Description**

Transect Number	**The of Number Pixel**	**Location**	**Description**	**Number of Corresponding points**
1	304	runs from south to north	perpendicular to the shore	238
2	175	runs from south east to north west	perpendicular to the shore	140
3	353	runs from north to south	perpendicular to the shore	339
4	169	runs from south west to north east	across to the shore with angle of 45^0	67
5	100	runs from south to north	perpendicular to the shore	52

3.4.2 Calculate the Predicted Absolute Bathymetry

The ground truth data was included to derive the absolute bathymetry. Therefore, linear regression was used with the relative ratio results and ground truth (DEM) values through five transects for each bands' ratio. The product is 25 linear regression solutions as shown in Figure 3.9. Each linear regression result provided the m_1, m_0 which were used to perform the (Stumpf et al. 2003) algorithm in Equation 3.8 to derive the absolute bathymetry for bands ratio:

$$Z = m_1 \frac{1n\left(nR_w(\lambda_i)\right)}{1n\left(nR_w(\lambda_j)\right)} - m_0 \qquad \textbf{3.8}$$

The five ratios were derived using the middle part of Equation 3.8. However, the result of the linear regression for each bands ratio against ground truth was also used to derive the second part of Equation 3.8. m_1, m_0, in Figure 3-9 : The Linear Regression for the Reflectance Ratio between Coastal and Yellow Bands and Ground Truth (DEM) in Transect 1 the given equation from the linear regression is: (y = -122.4*x + 168.42).

Therefore, m_1 = -122.4. And m_0 = 168.42, where (x) is the ratio between coastal and yellow bands along Transect 1.

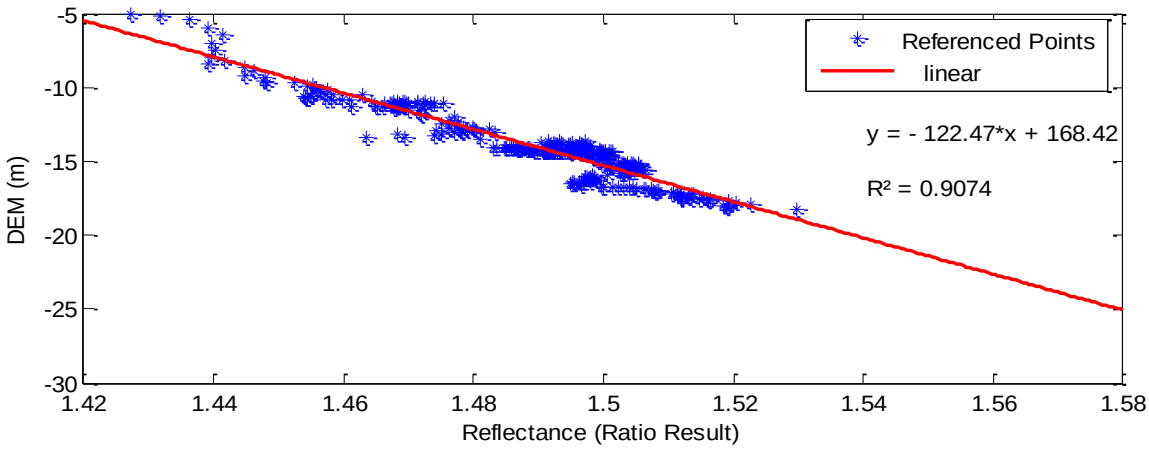

Figure 3-9 : The Linear Regression for the Reflectance Ratio between Coastal and Yellow Bands and Ground Truth (DEM) in Transect 1

Chapter Four: **Results and Discussion**

The main objective of this research thesis is to drive bathymetry measurements using Worldview-2's new coastal blue band in combination with the other four visible bands (blue, green, red, and yellow). The relative bathymetry and the predicted absolute bathymetry were obtained using the Ratio transform method. Then statistical analysis methods were performed to define the most ideal band ratios for the best penetration range.

4.1 The Results of Relative Bathymetry

In this section, five combinations of ratios between reflectance bands were obtained using the first part of (Stumpf et al. 2003) ratio algorithm as shown in Equation 4.1.

$$Z = \frac{1n\left(nR_w(\lambda_i)\right)}{1n\left(nR_w(\lambda_j)\right)} \qquad \textbf{4.1}$$

Where $R_w(\lambda_i)$ is the reflectance of the first band and, and $R_w(\lambda_j)$ is the reflectance of the second band. This ratio method was based on the rate of absorption. One of the essential uses of this method is to remove the effects of varying albedo at the bottom of the water and to make both bands affected in similar ways. Therefore, the band with the higher absorption degree decreases consistently faster while the depth increases. The ratio increases when the depth increases and as result, the ratio between these bands is determined to be affected by the increase of the depth more so than the varying of bottom albedo.

(Stumpf et al. 2003) used only one combination of ratio in his research work—blue and green bands. However, Madden's (2011) research sought to evaluate the contribution of the new yellow band by combining the ratio of the yellow band with blue, green, and red bands. Thus, Madden compared his three ratios to the ratio that (Stumpf et al. 2003) used, which is blue and

green ratio. He obtained greater accuracy by using the combinations with a yellow band compared to just blue and green bands.

The evaluation of the Coastal blue band was one of the research objectives. Therefore, five combinations ratios of new Coastal blue band with other four visible bands such as blue, green, yellow, and red were done in the methodologies section. Finding the best band ratio to determine the penetration range was also one of the objectives.

Figure **4-1**, Figure **4-2**, Figure **4-3**, Figure **4-4** and Figure **4-5** are the results of the relative bathymetry performance.

Figure 4-1 represents the ratio between the blue and green band and represents the ratio which (Stumpf et al. 2003) used to perform his algorithm. This ratio was used in this research as a comparison to the new coastal blue band ratios combinations. Qualitative methods were used to differentiate between these ratios combinations as follows in next section

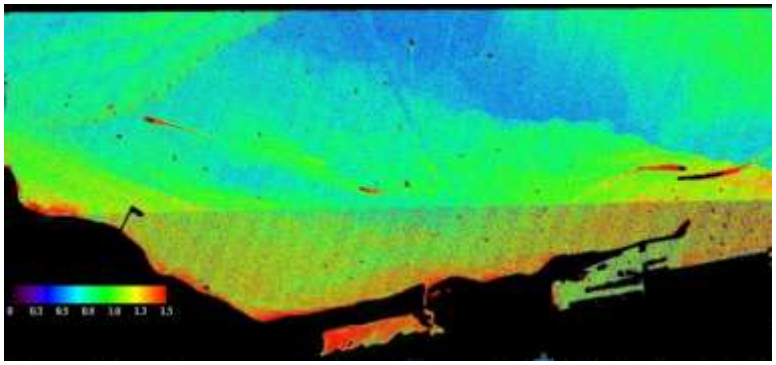

Figure 4-1: The Reflectance Ratio between Blue and Green Bands

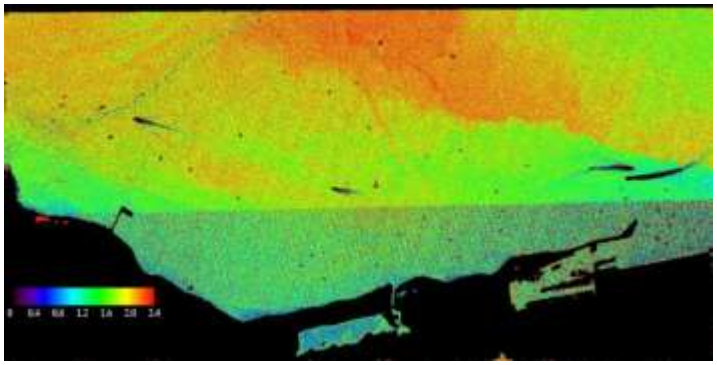

Figure 4-2: The Reflectance Ratio between Blue and Coastal Blue Bands

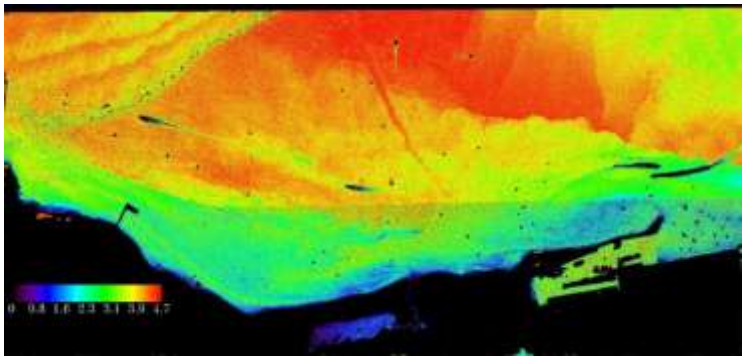

Figure 4-3: The Reflectance Ratio between Red and Coastal Blue Bands

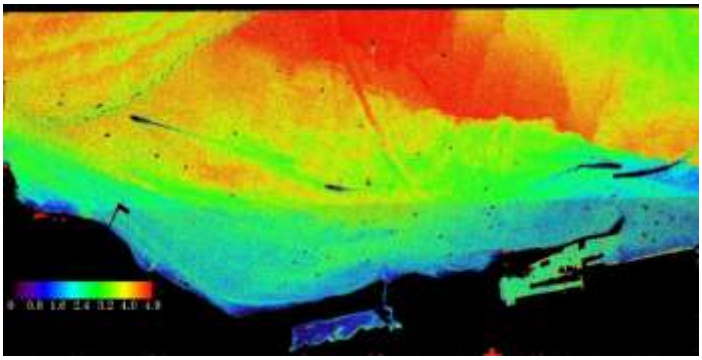

Figure 4-4: The Reflectance Ratio between Green and Coastal Blue Bands

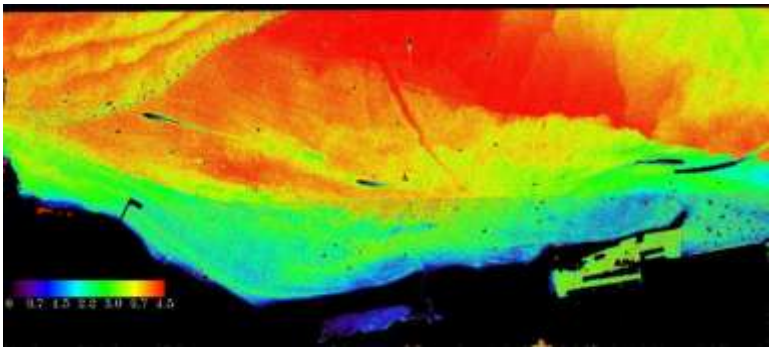

Figure 4-5: The Reflectance Ratio between Yellow and Coastal Blue Bands

The ratio between the yellow and costal blue bands helps distinguish various topographic features beneath the deep water. The gradual change in color indicates the gradual change in depth. After comparing the ratio results of the bands found in above, the ratio of yellow and coastal blue bands indicates a higher correlation with water depth, particularly in shallow water areas. Furthermore, the delineation of the shoreline has more correlation with this ratio since most of the dark blue color is clear with a range between 0.0-4.5. As the area of water becomes deeper, the color becomes darker, such as the blue (0.6-2.2), green (2.2-3.0), yellow (3.4-3.7), and red (3.7-4.5) parts of the image which represent the ratio depth between different bathymetric areas as seen in Figure **4-5**.

4.2 The Results of Absolute Bathymetry

The predicted absolute bathymetry was obtained using five transects. The transects served as an ideal means by which the same corresponding (reference) points could be extracted between the ground truth (DEM) data and the results of the relative bathymetry, which is the Band-ratio combinations (Madden 2011). Therefore, 25 linear regression plots were obtained to define this relationship between the ground truth (DEM) data and the relative bathymetry. Then, the predicted absolute bathymetry for all of the Band-ratio combinations was calculated via these 25 linear regressions.

The results of the relative bathymetry gave indication for the yellow and coastal blue ratio to be the optimum ratio. However, this is based on visual assessment. Therefore, the absolute bathymetry calculated based on linear regression method, which is important to evaluate the correlation between each ratio and the ground truth (DEM) data.

4.2.1 The linear regression results for the yellow and coastal blue ratio against DEM.

The linear regression between each ratio combination and ground truth (DEM) data has 25 results (plots). The results of Coastal blue and yellow ratio bands have a high correlation with ground truth (DEM) data. Therefore, the result of relative bathymetry for the ratio between Coastal blue and yellow bands against ground truth (DEM) data is expressed in the five figures below. However, the rest of the 25 linear regression results can be found in the appendix section.

The coefficient of determination in Figure **4-10** is approximately 93%, which indicates that most of the referenced points along transect 5 are very similar to the ground truth data. As a result, the ratio between yellow and coastal blue bands successfully met the objectives through transect 5. Also, through Transect 3, as shown in Figure **4-8**, the coefficient of determination value is

approximately 91 %, so most of the referenced points along Transect 3 are very similar to the ground truth data. Furthermore, Figure **4-6**, and Figure **4-7** show the coefficient of determination values through Transect 1 and Transects 2, respectively. The ratio derived the bathymetry for more than half of the corresponding points accurately. However, the coefficient of determination value along Transect 4 was approximately 27 % which indicates that most of the referenced points along Transect 4 are not similar to the ground truth data as shown in Figure **4-9**. Consequently, the ratio between yellow and coastal blue bands did not produce most of the bathymetric information through Transect 4 correctly.

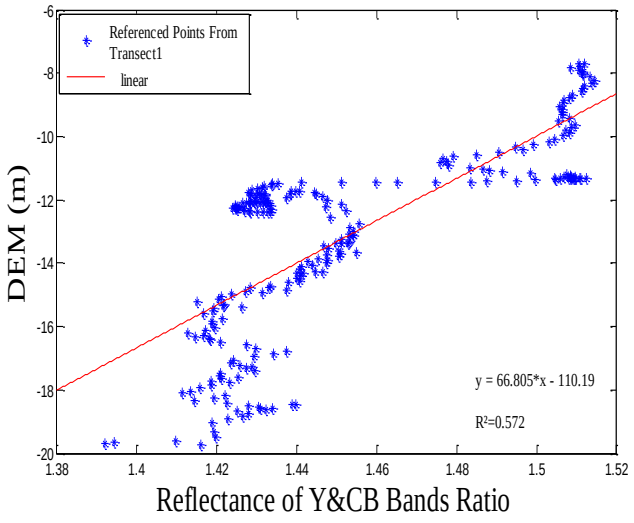

Figure 4-6: The Reflectance Ratio between Coastal Blue and Yellow Bands

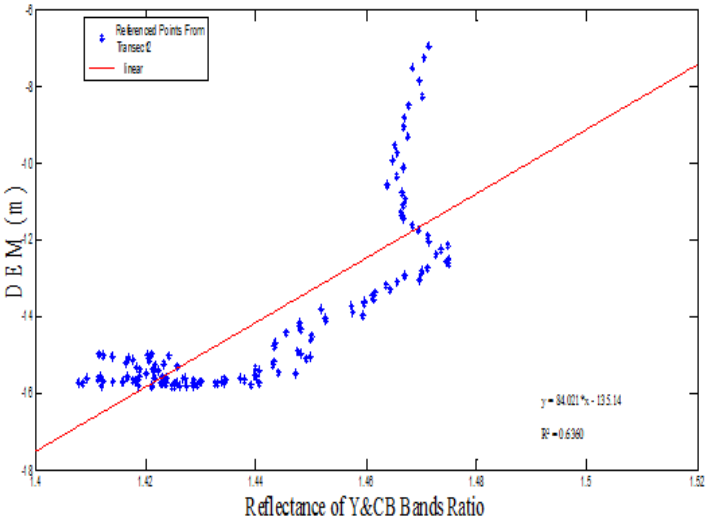

Figure 4-7: The Reflectance Ratio between Coastal Blue and Yellow Bands

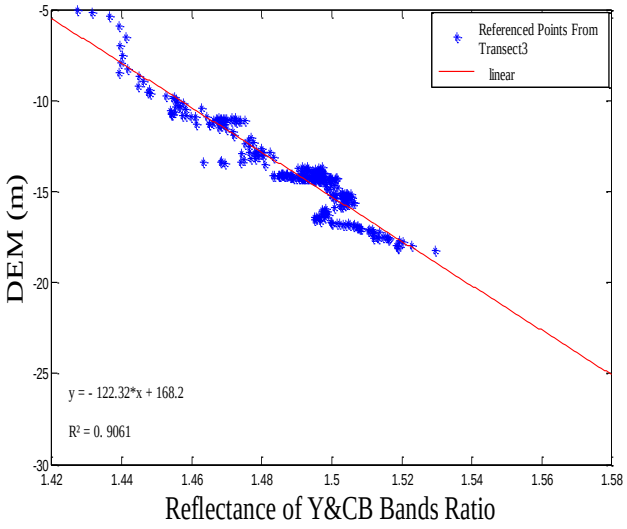

Figure 4-8: The Reflectance Ratio between Coastal Blue and Yellow Bands

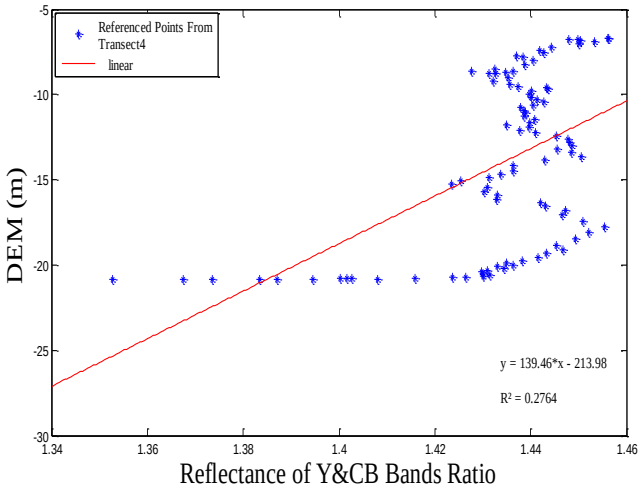

Figure 4-9: The Reflectance Ratio between Coastal Blue and Yellow Bands

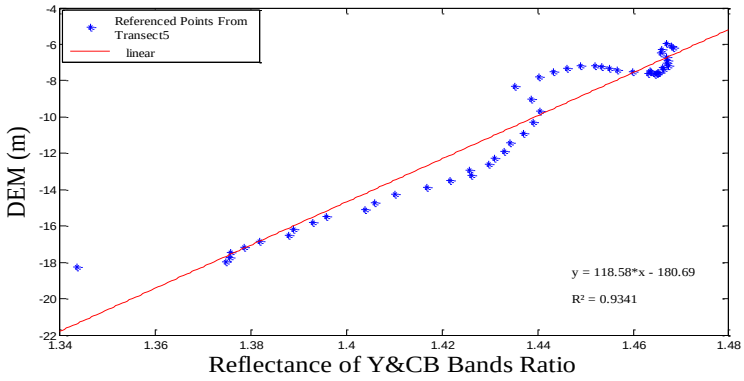

Figure 4-10: The Reflectance Ratio between Coastal Blue and Yellow Bands

4.2.2 The predicted absolute bathymetry Compared to The Ground Truth (DEM)

The following transects illustrate the similarities and differences between the absolute bathymetry for each of the five ratio combinations and the ground truth through all five transects. Moreover, the following shows the coefficient of determination value for each ration.

4.2.3 Transect 1

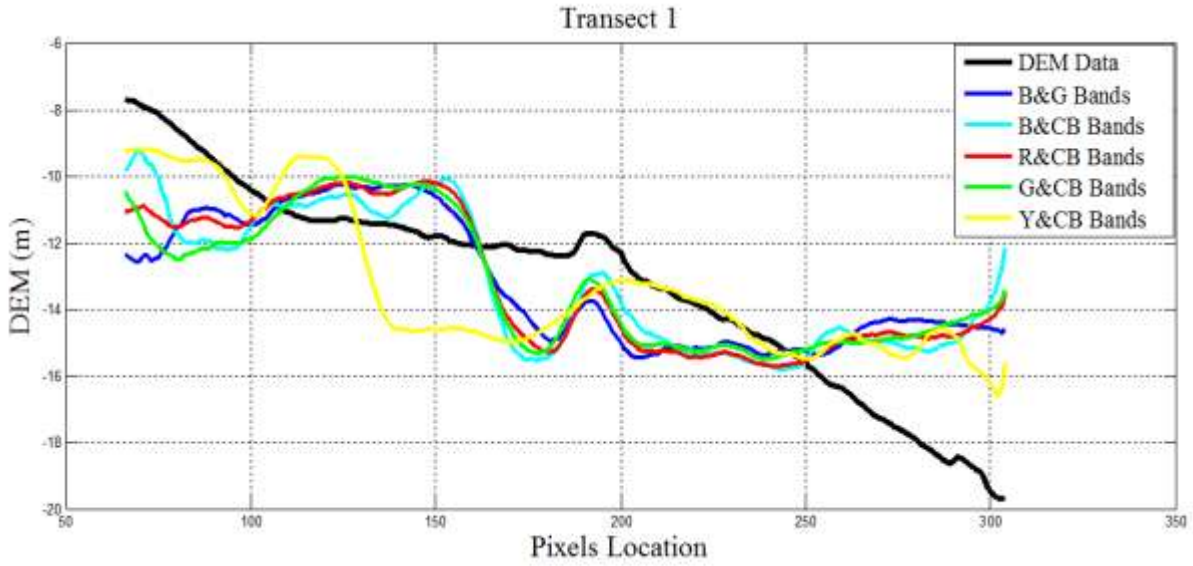

Figure 4-11: Absolute bathymetry compared to the DEM. The solid lines are the running mean of each data set along Transect 1 to smooth the data.

The ratio combinations Through Transect 1	**B&G**	**B&CB**	**R&CB**	**G&CB**	**Y&CB**
The Square of correlation coefficient values	**0.4103**	**0.5107**	**0.445**	**0.4895**	**0.572**

In Figure 4-11, all ratio combinations overestimated the depth for the first 50 pixels except the yellow and coastal blue ratio. This could be because of pollution occurring in the port area or from the influence of low albedo, which reduces the blue/green band reflectance occurrence in the reef area (Madden 2011). The yellow and coastal blue ratio was similar to the DEM between pixels number 210 to 230. Also, between pixel numbers 108 to 250 all of the ratios were almost similar for estimating the depth except yellow and coastal blue bands ratio. This ratio

underestimates the depth between pixel numbers 108 to 130. Although, there is a noticeable drop it overestimates the depth between pixel numbers 130 to 200. However, the yellow and coastal blue bands ratio was almost similar to the depth captured at pixel numbers 205 to 250. It is clear that the red and coastal blue and the green and coastal blue bathymetry have almost similar profiles along Transect 1. Moreover, these two combinations and the green/blue are the closest ratios to the DEM when Transect 1 occurs over dark bottom type (Madden 2011). The blue and coastal blue ratio has more errors compared to the DEM. According to Madden (2011), this could be because of the influence of lighter sand or reef segments. The yellow and coastal blue bands report the deepest drop in depth (16 m) at the end of Transect 1.

4.2.4 Transect 2

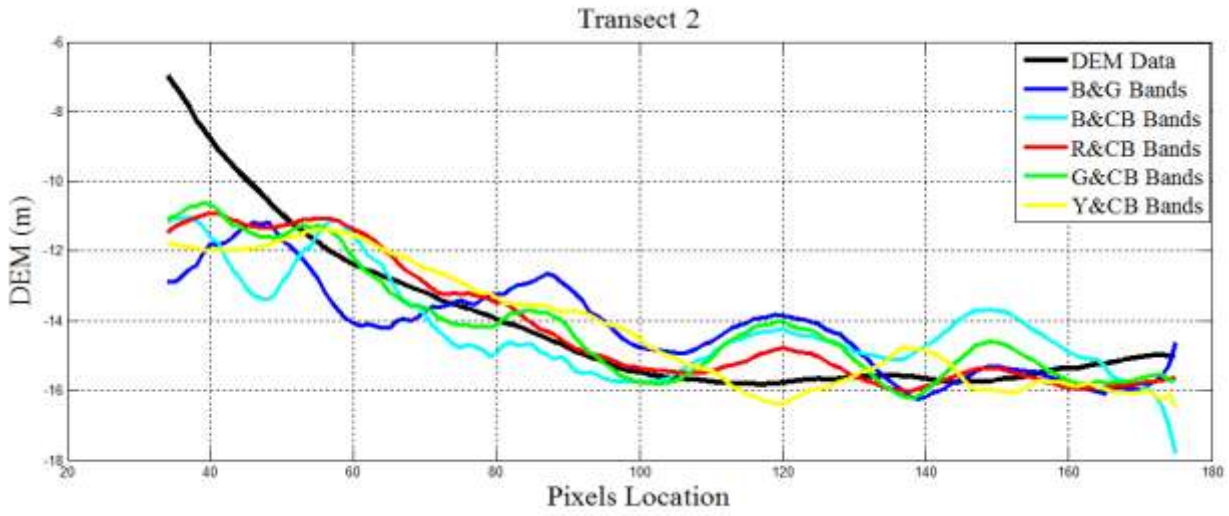

Figure 4-12: Absolute bathymetry compared to the DEM. The solid lines are the running means of each data set a long Transect 2 to smooth the data.

The ratio combinations Through Transect2	**B&G**	**B&CB**	**R&CB**	**G&CB**	**Y&CB**
The Square of correlation coefficient values	**0.4087**	**0.5344**	**0.7192**	**0.6782**	**0.6360**

In Figure 4-12 all of the five ratios overestimate the depth from the start of Transect 2 until up to number 50. It is obvious that the red and Coastal Blue bands ratio was constant and almost the same over Transect 2, starting from pixel location 80. However, there were no corrections from the beginning of Transect 2 until point number 80. The higher correlation between the DEM and the ratio combinations occurred with the red and Coastal blue and the green and Coastal blue. However, the blue and Coastal blue band dropped and provided the highest depth at the end of Transect 2 reaching 17m at pixel number 170.

4.2.5 Transect 3

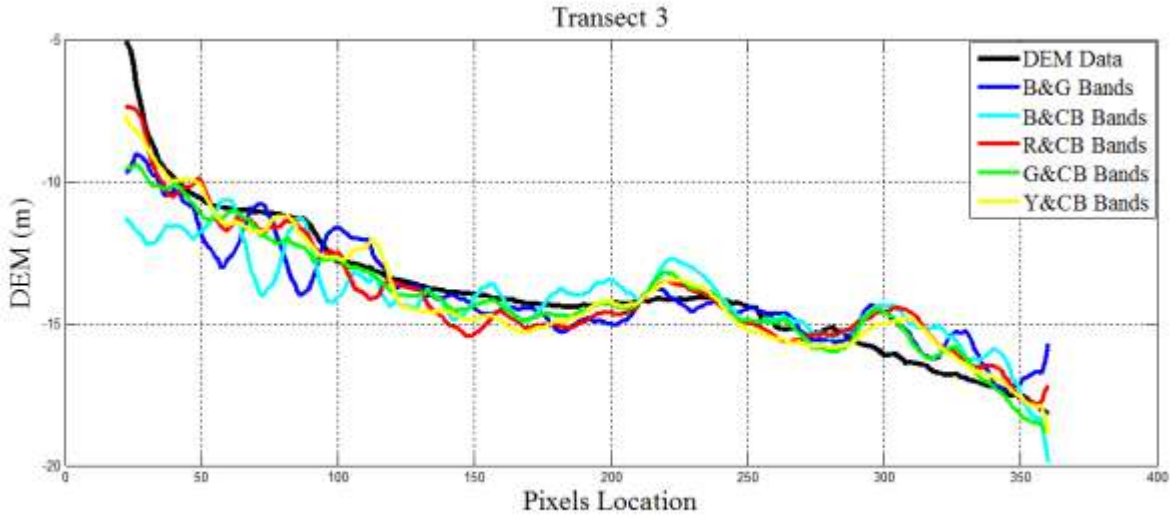

Figure 4-13: Absolute bathymetry compared to the DEM. The solid lines are the running mean of each data set along Transect 3 to smooth the data.

The ratio combinations Through Transect 3	**B&G**	**B&CB**	**R&CB**	**G&CB**	**Y&CB**
The Square of correlation coefficient values	**0.7833**	**0.6616**	**0.8660**	**0.8917**	**0.9061**

The derived bathymetry profiles for most of the ratios, as shown in Figure 4-13, gave a good correlation over all in Figure 4-13. It is obvious that the yellow and Coastal blue bands have the highest correlation with the DEM in most portions of Transect 3 as the correlation value was 0.9061. Additionally, the blue and green band provided a good correlation with the DEM producing a value of 0.7833. According to Madden (2011) the green and blue band does not influence with lighter sand. Like Transect 2, the blue and Coastal blue band reports its deepest

depths over Transect 3 reaching 19 m at pixel 362.The red and Coastal Blue ratio derived bathymetry similar to the DEM in most of Transect 3 portions. Furthermore, the red and Coastal blue ratio, and green and coastal blue ratio are almost the equivalent for retrieving the depth along Transect 3. In conclusion, the yellow and coastal blue band ratio had the highest correlation with the DEM with overlapping between green and Coastal blue and green and blue between pixel 300 and 320.

4.2.6 Transect 4

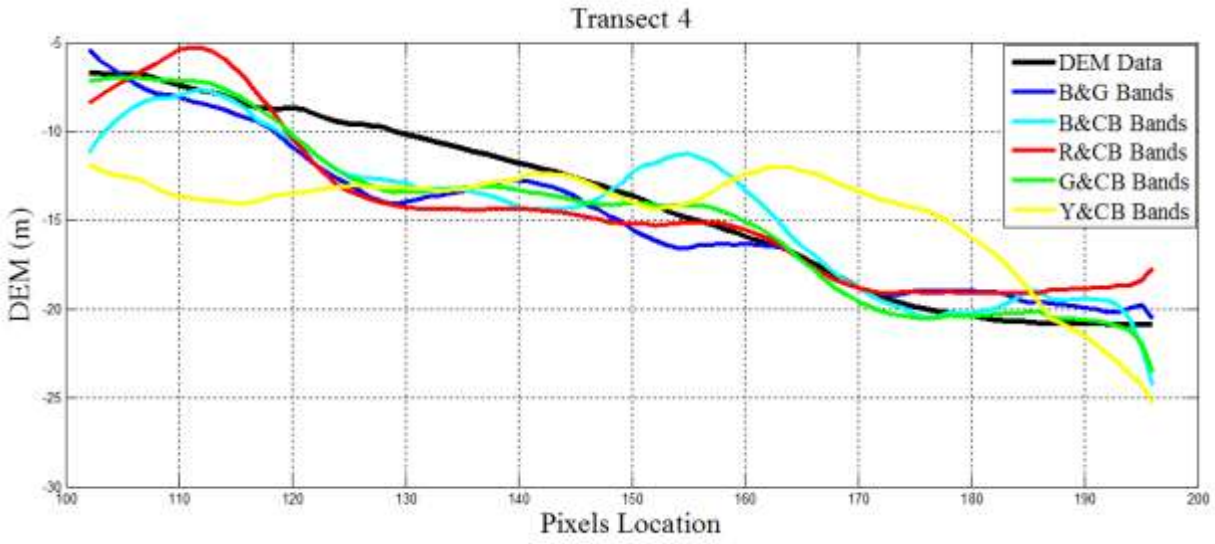

Figure 4-14: Absolute bathymetry compared to the DEM. The solid lines are the running mean of each data set along Transect 4 to smooth the data.

The ratio combinations Through Transect 4	B&G	B&CB	R&CB	G&CB	Y&CB
The Square of correlation coefficient values	0.8793	0.7019	0.8155	0.9207	0.2764

Along Transect 4 in Figure 4-14 was the green and coastal blue derived bathymetry with the highest correlation when compared with the DEM since there was some overlapping in certain portions along transect 4. The similarity between red and coastal blue and blue and green is clear along when observed most of the Transect 3 portions, especially between pixel 170 and pixel 180. Furthermore, these ratios were the second highest correlation after green and Coastal blue.

The derived bathymetry from yellow and Coastal blue along Transect 4 differed from all five transects, as it gave an unexpected value of 0.2764. Thus, there was noticeable error through this transect when compared to DEM. The value of the yellow and Coastal blue ratio was almost constant from the beginning of Transect 4 up to pixel 160 and provided the deepest depth along Transect 4.

4.2.7 Transect 5

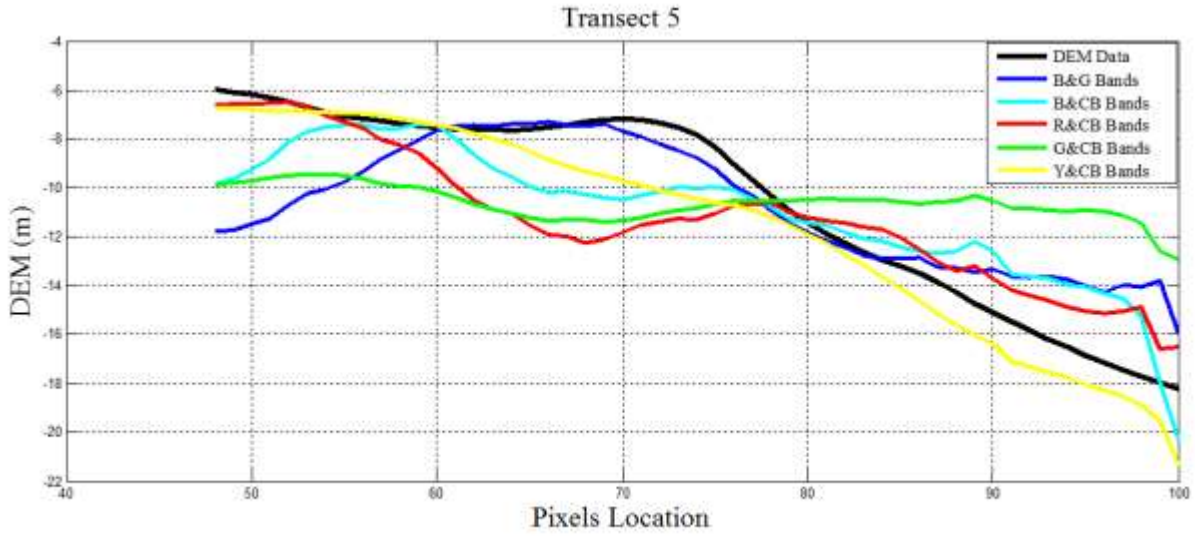

Figure 4-15: Absolute bathymetry compared to the DEM. The solid lines are the running mean of each data set along Transect 5 to smooth the data.

The ratio combinations Through transect 5	B&G	B&CB	R&CB	G&CB	Y&CB
The Square of correlation coefficient values	0.4178	0.4169	0.5285	0.0450	0.9341

From Figure 4-15 the derived bathymetry profile of yellow and Coastal blue has the highest correlation with the DEM along Transect 5. There was also overlapping between this ratio and the DEM from pixel 55 to 61. In addition, yellow and coastal blue provided the deepest depth as it dropped to 18m at the end of Transect 5.The derived bathymetry from green and Coastal blue was almost constant along Transect 5. However, this ratio failed to retrieve the depth along Transect 5. The blue/green and blue/coastal blue ratios provide almost equal correlations with the

DEM along this transect, however, the blue and green ratio overlapped with the DEM between pixel numbers 60 to 68.

4.3 Assessment of Predicted Absolute Bathymetry Utilizing Statistical analysis techniques

The differences between the absolute bathymetry (predicted depth) and the DEM for each ratio bands through each transects were calculated by subtracting them. However, the mean, maximum and minimum values, as well as the standard deviation for each ratio from every transect was calculated to compare all of the ratio bands for their ability to derive the bathymetry as shown in Table **4-1**, Table **4-2**, Table **4-3**, Table **4-4**, and Table **4-5**.

Table 4-1: The Error Values of Predicted bathymetry utilizes Blue and Green ratio Combination.

Transect Number	Absolute Mean Value	Maximum Value	Minimum Value	Standard Deviation
1	4.32	5.23	-5.61	2.32
2	5.60	2.86	-6.02	1.70
3	4.68	2.61	-5.54	1.14
4	4.92	4.92	-4.09	1.71
5	6.15	6.38	-6.78	3.07

Table 4-2: The Error Values of Predicted bathymetry utilizes Coastal Blue and Blue ratio Combination.

Transect Number	Absolute Mean Value	Maximum Value	Minimum Value	Standard Deviation
1	2.79	7.59	-3.61	2.11
2	4.97	2.30	-4.97	1.51
3	6.42	2.32	-6.42	1.45
4	9.61	6.00	-9.61	2.67

Table 4-3: The Error Values of Predicted bathymetry utilizes Coastal Blue and Red ratio Combination.

Transect Number	Absolute Mean Value	Maximum Value	Minimum Value	Standard Deviation
1	2.02	6.33	-4.18	2.24
2	5.26	1.58	-5.26	1.17
3	3.15	2.31	-3.15	0.89
4	3.09	4.36	-3.99	2.12
5	1.95	6.30	-6.31	2.73

Table 4-4: The Error Values of Predicted bathymetry utilizes Coastal Blue and Green ratio Combination.

Transect Number	Absolute Mean Value	Maximum Value	Minimum Value	Standard Deviation
1	3.51	6.21	-3.67	2.15
2	4.55	2.04	-4.59	1.25
3	4.60	3.04	-4.76	0.88
4	0.88	2.51	-3.19	1.39
5	4.76	8.71	-4.78	3.89

Table 4-5: The Error Values of Predicted bathymetry utilizes Coastal Blue and Yellow ratio Combination.

Transect Number	Absolute Mean Value	Maximum Value	Minimum Value	Standard Deviation
1	1.49	4.47	-3.04	1.96
2	4.57	1.94	-4.57	1.34
3	1.34	2.62	-2.11	0.73
4	4.18	6.91	-6.23	4.19
5	0.76	1.60	-3.13	1.02

4.3.1 The Error Absolute Mean Values for the Predicted Bathymetry

The primary objective of this research is to define the optimum band rations, among five possibilities, for determining the bathymetry. Additionally, the contribution of the new coastal blue band to determine the penetration ranges will be evaluated. Therefore, the magnitude of the absolute mean of error in metres resulting from the difference between ground truth and predicted depth through all five transects is shown in Figure 4-16.

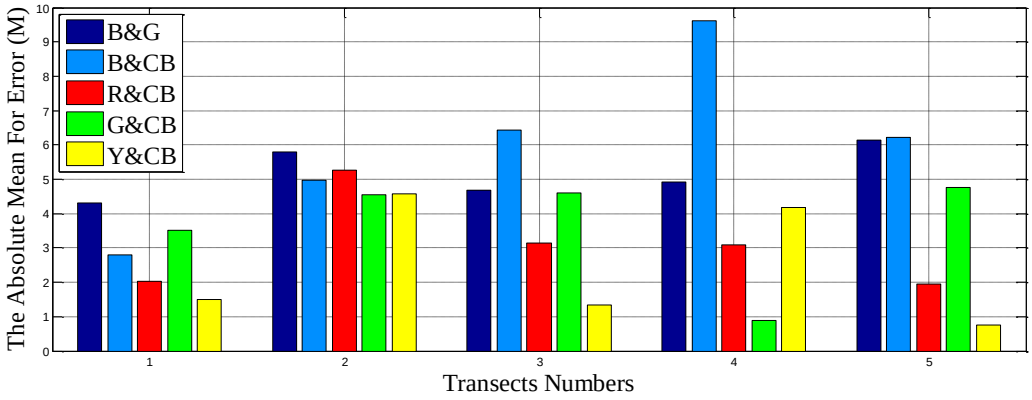

Figure 4-16: The mean values for error magnitude in metres

4.3.2 The Error Standard Deviation values for the Predicted Bathymetry

The chart in Figure 4-17 shows the standard deviation resulting from the difference between ground truth and the predicted depth through all five transects.

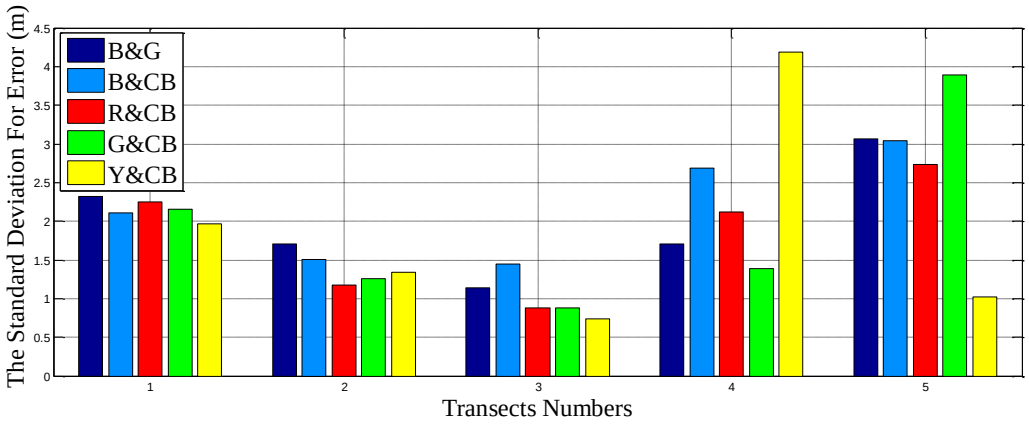

Figure 4-17: The standard deviation values

Based on the statistical analysis shown above, by contributing the new coastal blue band the accuracy of derived bathymetry was increased compared to (Stumpf et al. 2003) original blue and green ratio. The ratio between the coastal blue and the yellow band ratio shows a significant contribution to deriving the bathymetry with an absolute mean error range of 1 m in Transect 1, 3, and 5. However, in Transect 2 and 4 the magnitude of error increased because of the change in the sea bed properties (bottom type). Although the hypothesis presented by (Stumpf et al. 2003) is sound, the ratio algorithm could be used to derive bathymetry independently from the substrate albedo (bottom type). The coastal blue band is capable of improving the accuracy of derived bathymetry from WorldView-2 even without classifying the bottom type. Transect 4 and 2 have more error because of the effect of the sedimentary areas through which they travel. Figure 4-18 was the only sediment thickness map available for the study area (Survey 1997) and was Geo-

referenced to (UTM Zone 10 North) projection system. However, the five transects extracted from WV-2 imagery were overlaid on top of this map. Figure 4-18 is different from a bathymetry map in that a bathymetry map provides the height difference between the bottom of the water body and the surface of the water, or the sea level, while a sediment thickness map is the thickness of layer on top of the bedrock. In observable areas, very close to the shoreline, the sediment thickness was not determined.

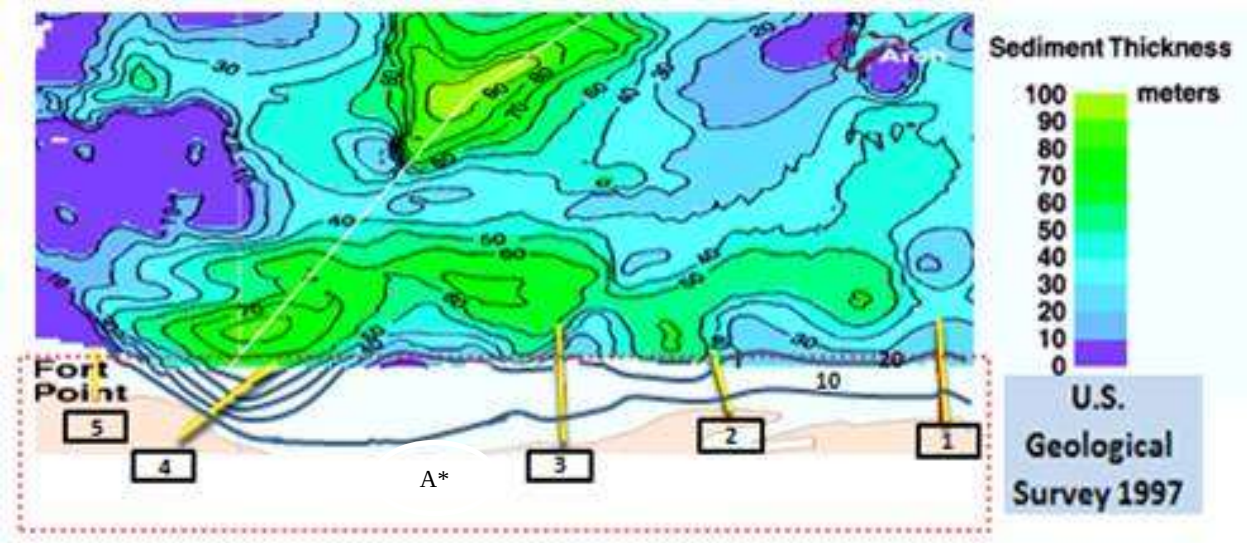

Figure 4-18: From right to left: Transect 1, Transect 2, Transect 3, Transect 4, and Transect 5. Box A* is hypothetical continuation of the contours lines.

Sediment consists of various elements which are transported by water such as solid particles of mineral and organic material (UNESCO and IRTCES 2011). The water reflectance was limited due to the effect of scattering and the absorption properties of the sediment types. The sediment layers limit the light penetration from the bottom of the water (Novo et al. 1989) because of a

sediment phenomenon that causes water turbidity and limits the light penetration and reflectance while excluding the growth of healthy plants on the ocean bed (UNESCO and IRTCES 2011). After analyzing the impact of sedimentary thickness on the accuracy of derived bathymetry from Figure 4-18 we observed that Transect 4 was influenced by the sediment since it was receding quickly into the deep sediment of 70 m. According to Figure 4-16 the absolute mean of error reached 5 m. Therefore, the accuracy of this transect was the most negatively affected compared to the other four. Transect 2 was the second worst accuracy as it receded very rapidly into the deep sediment of 40 m. As a result the absolute mean of error was 5 m as shown in Figure 4-16 . However, Transect 1 provided good accuracy since it occurs in a shallow sedimentary area with a thickness of 20 m, resulting in an absolute mean of error of 1 m as shown in Figure 4-16. Transect 5 delivered accurate results as well since it occurred in a very shallow area close to the bedrock. As a result the absolute mean of error was 1 m as shown in Figure 4-16. Transect 3 provided the single best accuracy as it travelled through a shallow sedimentary are with a thickness of 10 to 30 m—until the last few pixels which hit 50 m of sedimentary thickness. As a result the absolute mean of error was 1 m as shown in Figure 4-16.

Chapter Five: **Conclusion**

The purpose of this research work was to evaluate the contribution of worldview-2 imagery for determining bathymetry applications. The research work was conducted over the west bay region of the San Francisco Bay. This place was chosen because of the availability of three difference data including the Worldview-2 imagery, Sonar data, and Sediment thickness map. Ratio transform method was used to obtain the bathymetry. A complete assessment of the Coastal blue band with other multi-spectral bands such as blue, green, yellow, and red bands was conducted using the relative ratio bathymetry method, which is based on the ratio between two reflectance bands with different in wavelength. The predicted depth was obtained in three phases, which included the spectral correction for WV-2 data, extracted water bodies through the elimination of non- water classes, and finally the (Stumpf et al. 2003) algorithm used to calculate the predicted depth. This depth was reached in two stages. The first represents the relative bathymetry and the second the absolute bathymetry. The linear regression between the relative bathymetry results obtained and the ground truth were calculated to produce the predicted bathymetry through five transects. The magnitude of all errors was calculated by subtracting the predicted depth from the ground truth depth in order to yield the absolute mean of error.

The results showed that the combination ratios between the Coastal blue band and the other three visible bands such as red, green, and yellow, had less error when compared to the blue and green ratio. However, the Coastal blue and blue band ratio had more errors over the blue green ratio because of the wavelength of the Coastal blue band and blue band are very close. Moreover, the ratio between the yellow and Coastal blue bands was the best choice of the other ratios as the average of the absolute mean error through all transects is about 1 m compared to the other

ratios. However, in Transect 2 and 4 this ratio had significant degradation in accuracy because of the changes in the bottom type and water properties, as these transects occur in thick sediment areas. Therefore, the ratio between the yellow and Coastal blue can be used for modeling the seafloor bed. This will be a very useful tool for users in terms of cost and time.

There are some recommendations for other research to take place such as utilizing ground truth areas with depth less than 8 meter. The worldview-2 has ability to determine depth up to 20 m (Globe 2010) . However, the ground truth depths in this research work were not less than 8 m, which forced this research to choose the corresponding points between the Worldview-2 data and the ground truth data in the range of 8 meters to 20 meters. Therefore, the availability of ground truth with depth less than 8 meter might also improve the accuracy as there will be additional of depth variation. Moreover, it is noticeable that some of the ratio combination either overestimated or underestimated the ground truth depth. Therefore, a weight might be added to the algorithm as well. The bottom type information data was not available for this research work. Therefore, this information should be included especially for having more detailed analysis. This information should be about the characteristics of each band with different bottom types such as sand, sea grass, etc. Furthermore, utilizing the bottom type data, which will allow to obtain information about the influence of each band corresponding to this bottom type variation. Moreover, a classification technique could be performed to improve the accuracy by separating each of the bottom types such as sand, grass etc. and then conducting the best method for each type. Modifications to the algorithm could be applied in order to combine a three bands' ratio instead of two. Also, having another stereo pair of Worldview-2 data for the same study area can help to generate 3D model for the shorelines. Furthermore, the quick revisit time that

Worldview-2 satellite has makes the water change detection research one of the important application Worldview-2 imagery has.

References

Alsubaie, N., M. Elhabiby and N. El-Sheimy (2012). The Potential of Using Multi-Spectral Satellite Imagery for Shallow Water Bed Mapping. . The Seventh National GIS Symposium Saudi Arabia 13.

Bierwith, P. N., T. Lee and R. V. Burne (1992). Shallow sea-floor reflectance and water depth derived by unmixing multispectral imagery. The First Thematic Conference on Remote Sensing for Marine and Coastal Environments. New Orleans, Louisiana: 8.

Camacho, M. A. (2006). Depth Analysis of Midway Atoll using QuickBird Multi-Spectral Imaging over Variable Substrates. Naval Postgraduate School. MONTEREY, CALIFORNIA. Master: 91.

D.Parthish, G.Gopinath and S.S.Ramakrishnan (2011). Coastal Bathymetry by COASTAL BLUE: 9.

Densham, M. P. J. (2005). Bathymetric mapping with Quickbird data

Dept. of Physical Oceanography, Naval Postgraduate School. Master.62.

DFTC (2012). Worldview-2 image. D. Globe, Data Fusion Technical Committees. IEEE.

Elsharkawy, A., M. Elhabiby and N. El-Sheimy (2012). Quality Control on the Radiometric Calibration of the WorldView-2 Data. Global Geospatial Conference 2012 (GSDI). Québec: 13.

Globe, D. (2010). the Benefits of the 8 Spectral Bands of WorldView-2, Digital Globe .12.

Gonzalez, R. C. and R. E. Woods (2002). Digital Image Processing, Prentice Hall.

Green, E. P., P. J. Mumby, E. A.J., C. D. Clark and E. A. J. Edwards) (2000). Remote sensing handbook for tropical coastal management. Paris.

Guenther, G. C., C. A.G., P. E. LaRocque and D. J. Reid (2000). Meeting the Accuracy Challenge in Airborne LiDAR Bathymetry. 20th EARSeL Symposium.

HAIBIN, S., H. LIU and W. D. HEYMAN (2008). "Automated Derivation of Bathymetric Information from Multi-Spectral Satellite Imagery Using a Non-Linear Inversion Model." Marine Geodesy 281–298(2008): 18.

Jensen, J. R. (1995). . Introductory Digital Image Processing : A Remote Sensing Perspective, Prentice Hall.

Lee, K. R., A. M. Kim, R. C. Olsen and F. A. Kruse (2011). Using WorldView-2 to determine bottom-type and bathymetry Ocean Sensing and Monitoring III. Orlando, Florida 8030:14.

Loomis, M. J. (2009). Depth Derivation from the Worldview-2 Satellite Using Hyperspectral Imagery. MONTEREY, CALIFORNIA, Naval Postgraduate School. Master: 69.

LYZENGA, D. R. (1985). "Shallow-water bathymetry using combined lidar and passive multispectral scanner data." INT. J. REMOTE SENSING 6: 12.

Madden, C. K. (2011). CONTRIBUTIONS TO REMOTE SENSING OF SHALLOW WATER DEPTH WITH THE WORLDVIEW-2 YELLOW BAND. MONTEREY, CALIFORNIA, Naval Postgraduate School. Master: 83.

Marchisio, G. F., Pacifici and C. Padwick (2010). On the Relative Predictive Value of the New Spectral Bands in the Worldwiew-2 Sensor. Geoscience and Remote Sensing Symposium (IGARSS) 2010 IEEE International25-30 July 2010. pp. 2723-2726.

McCarthy, B. L. (2010). Coastal Bathymetry Using 8-Color Multispectral Satellite Observation of Wave Motion. MONTEREY, CALIFORNIA, Naval Postgraduate School. Master: 71.

McFEETERS, S. K. (1996). "The use of the Normalized Difference Water Index (NDWI) in the delineation of open water features." International Journal of Remote Sensing. 17(7):1425-1432.9.

McNair, G. (2010). Coastal Zone Mapping with Airborne LiDAR Bathymetry. DEPARTMENT OF MATHEMATICAL SCIENCES AND TECHNOLOGY, NORWEGIAN UNIVERSITY OF LIFE SCIENCES. Master: 100.

Novo, E. M. L. M., J. D. Hansom and P. J. Curran (1989). "The effect of sediment type on the relationship between reflectance and suspended sediment concentration." International Journal of Remote Sensing 10:1283-1289: 8.

Stumpf, R., K. Holderied and M. Sinclair (2003). Determination of water depth with high-resolution satellite imagery over variable bottom types. the American Society of Limnology and Oceanography, Inc. 48(1): 547-556.

Survey, U. S. G. (1997, 10 October 2008). "Sediment Thickness in West-Central San Francisco Bay." Retrieved 14 September 2012.

Timothy, A., Kearns and J. Breman (2010). Bathymetry: the art and science of seafloor modeling for modern applications. ESRI: 36.

UNESCO and IRTCES (2011). Sediment Issues & Sediment Management in Large River Basins Interim Case Study Synthesis Report

International Sediment Initiative Beijing, UNESCO Office. Technical Documents in Hydrology: 88.

Updike, T. and C. Comp (2010). Radiometric Use of WorldView-2 Imagery. Longmont, Colorado, DigitalGlobe: 16.

APPENDIX

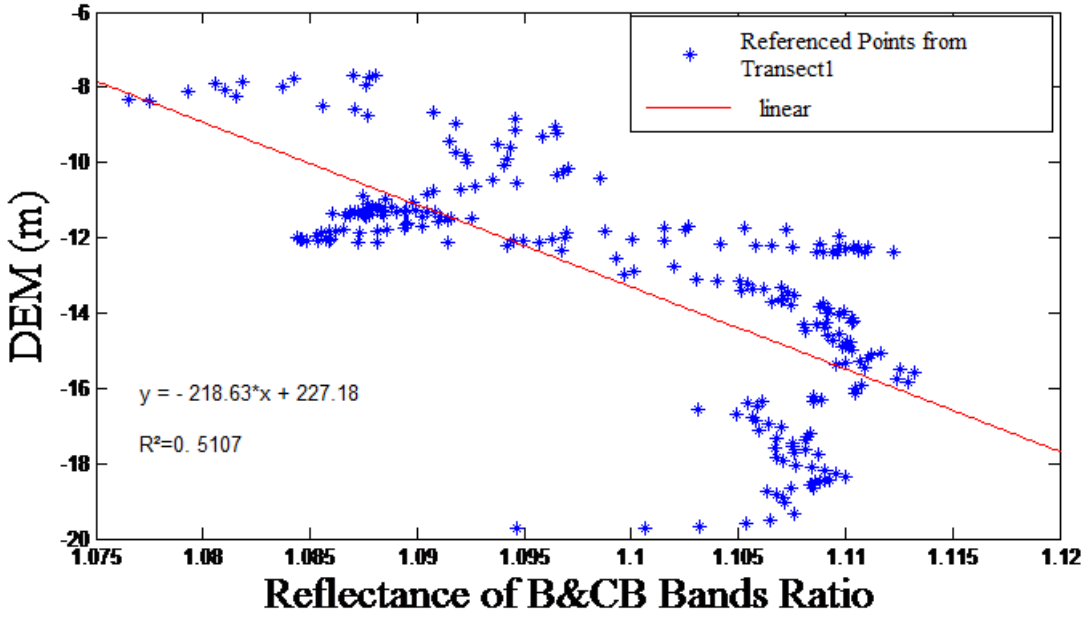

Figure A-1: Linear Regression for Blue/Coastal blue bands along Transect1. The x-axis is the ratio value and y- axis is the corresponding ground truth (DEM) Value at that pixel.

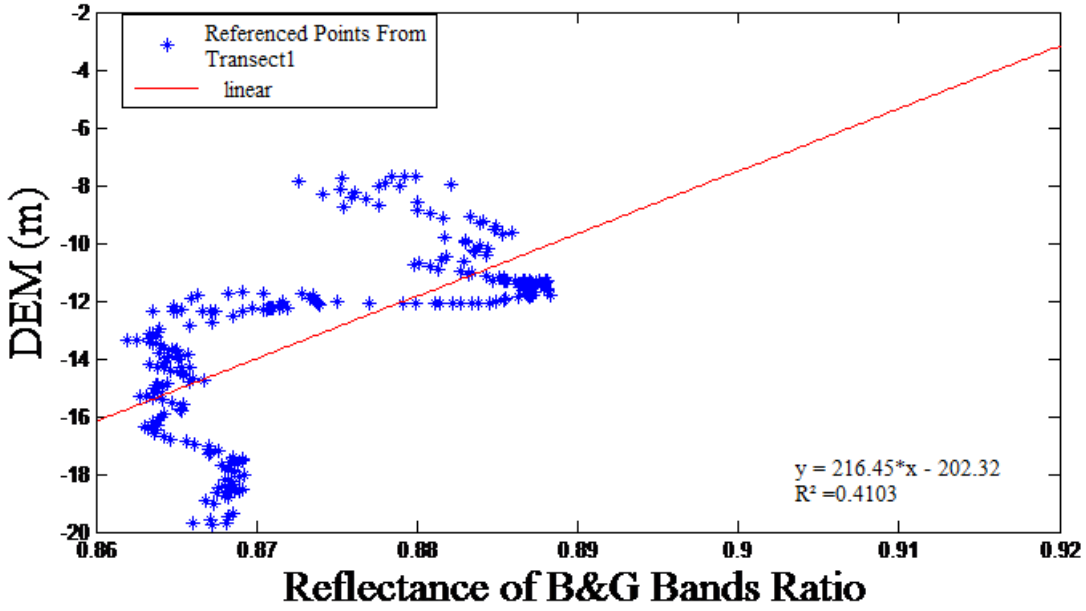

Figure A-2: Linear Regression for Blue/Green along bands Transect1. The x-axis is the ratio value and y- axis is the corresponding ground truth (DEM) Value at that pixel.

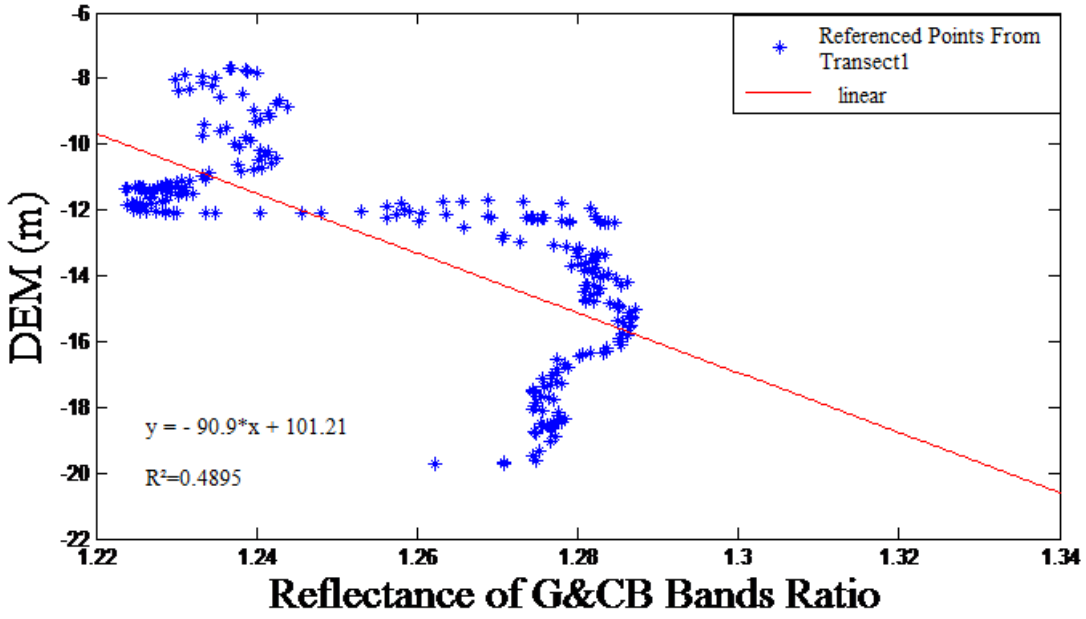

Figure A-3: Linear Regression for Green/Coastal blue bands along Transect1. The x-axis is the ratio value and y- axis is the corresponding ground truth (DEM) Value at that pixel.

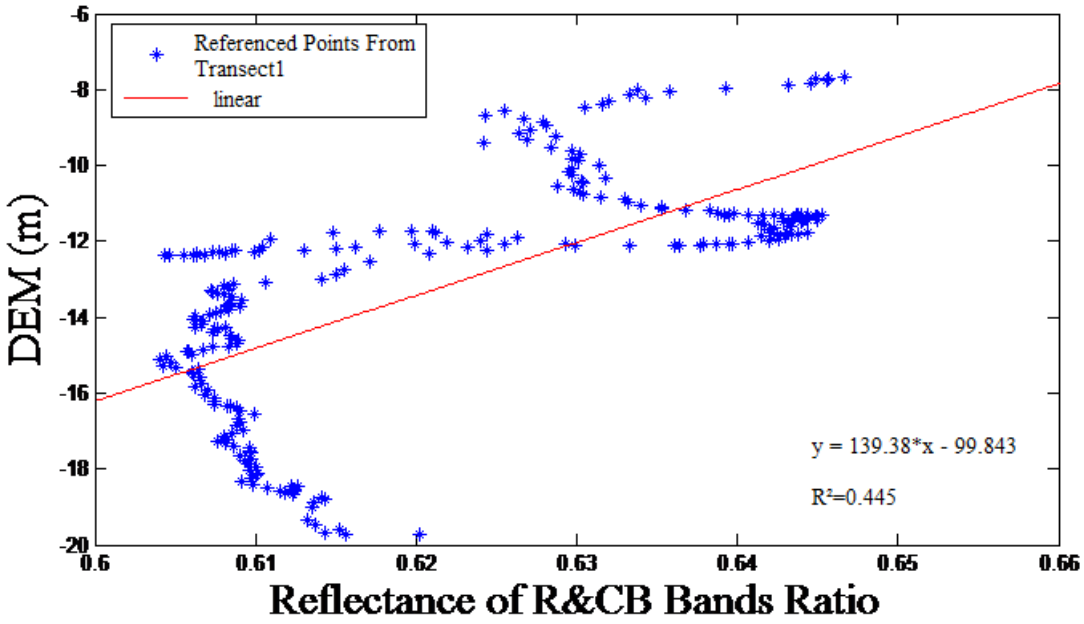

Figure A-4: Linear Regression for Red/Coastal blue bands along Transect1. The x-axis is the ratio value and y- axis is the corresponding ground truth (DEM) Value at that pixel.

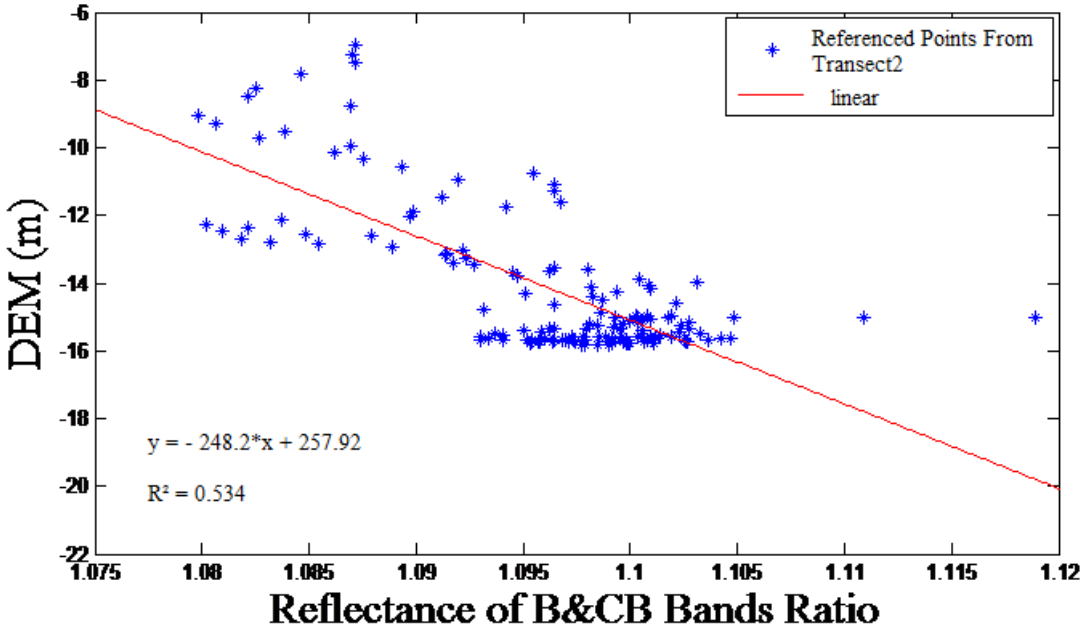

Figure A-5: Linear Regression for Blue/Coastal blue bands along Transect2. The x-axis is the ratio value and y- axis is the corresponding ground truth (DEM) Value at that pixel.

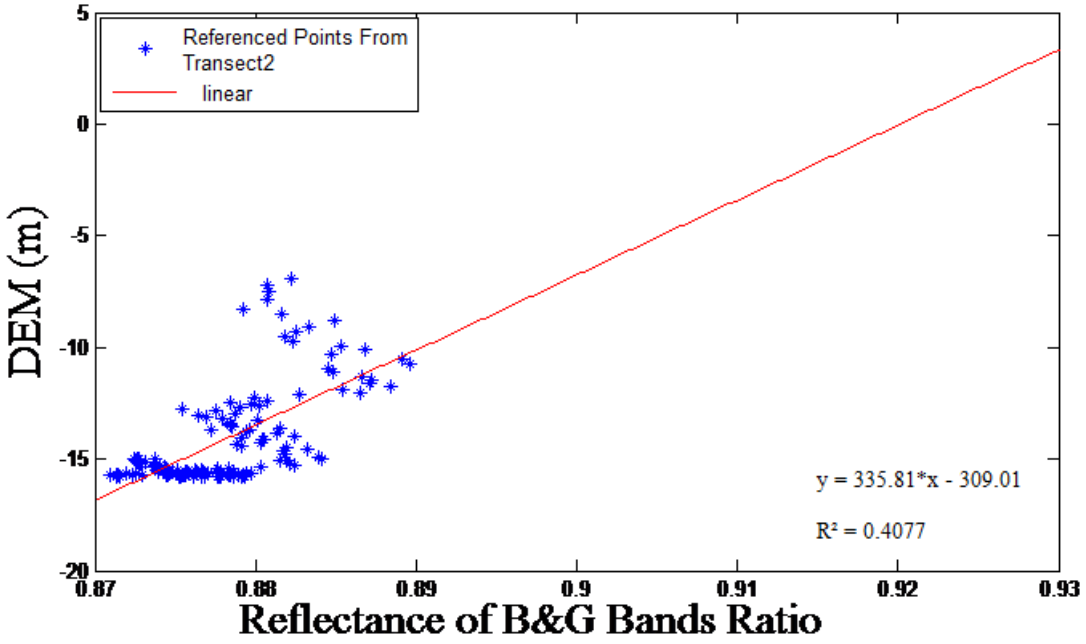

Figure A-6: Linear Regression for Blue/Green bands along Transect2. The x-axis is the ratio value and y- axis is the corresponding ground truth (DEM) Value at that pixel.

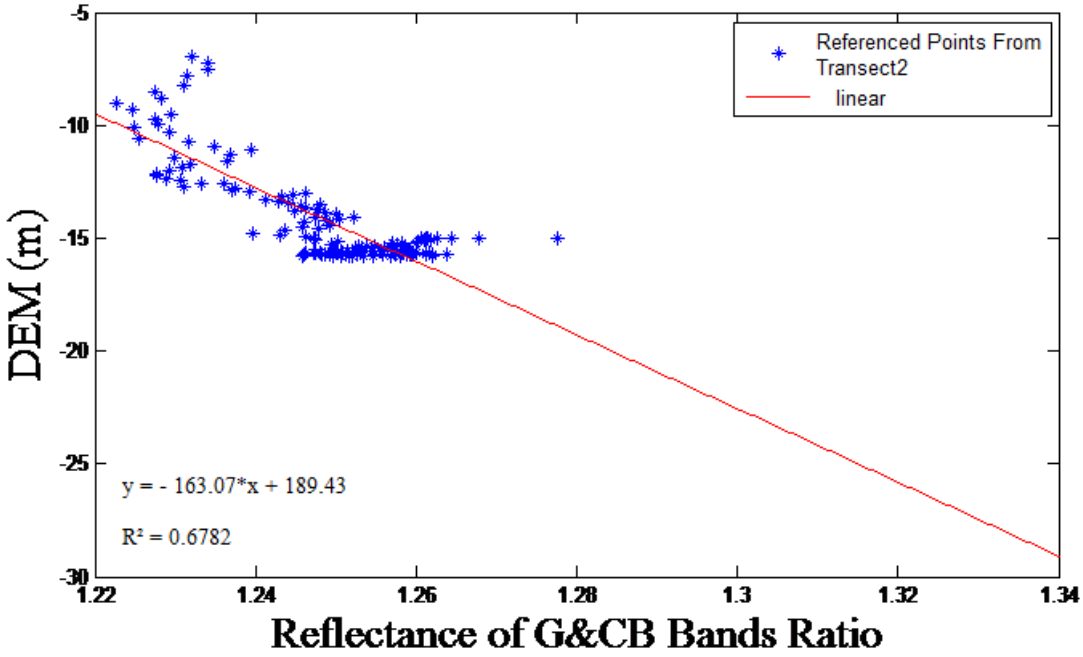

Figure A-7: Linear Regression for Green/Coastal blue bands along Transect2. The x-axis is the ratio value and y- axis is the corresponding ground truth (DEM) Value at that pixel.

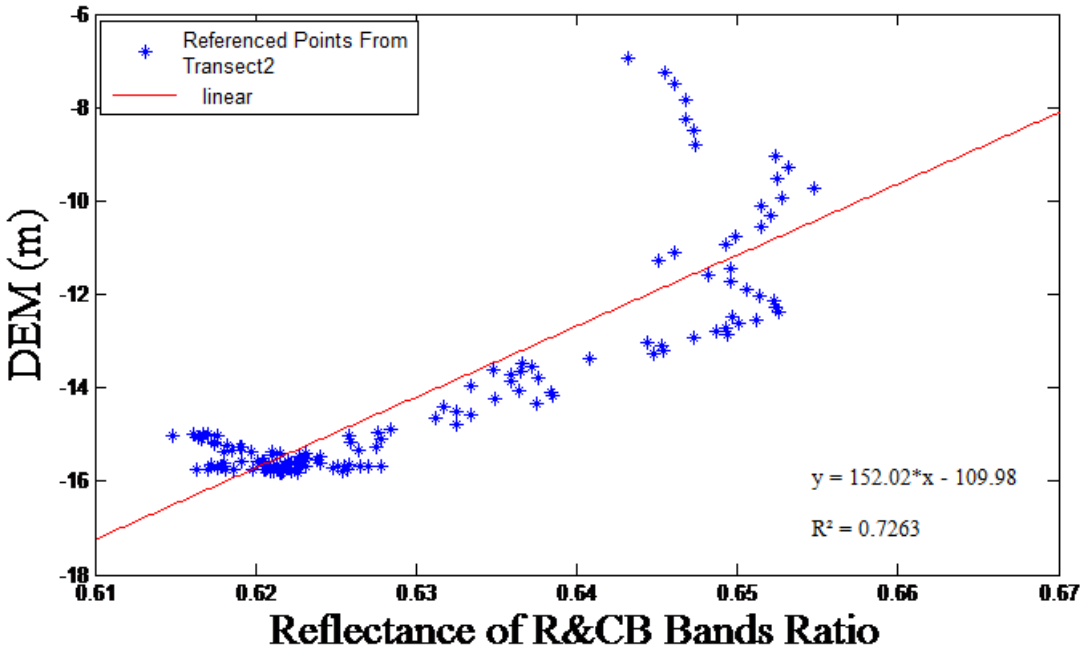

Figure A-8: Linear Regression for Red/Coastal blue along Transect2. The x-axis is the ratio value and y- axis is the corresponding ground truth (DEM) Value at that pixel.

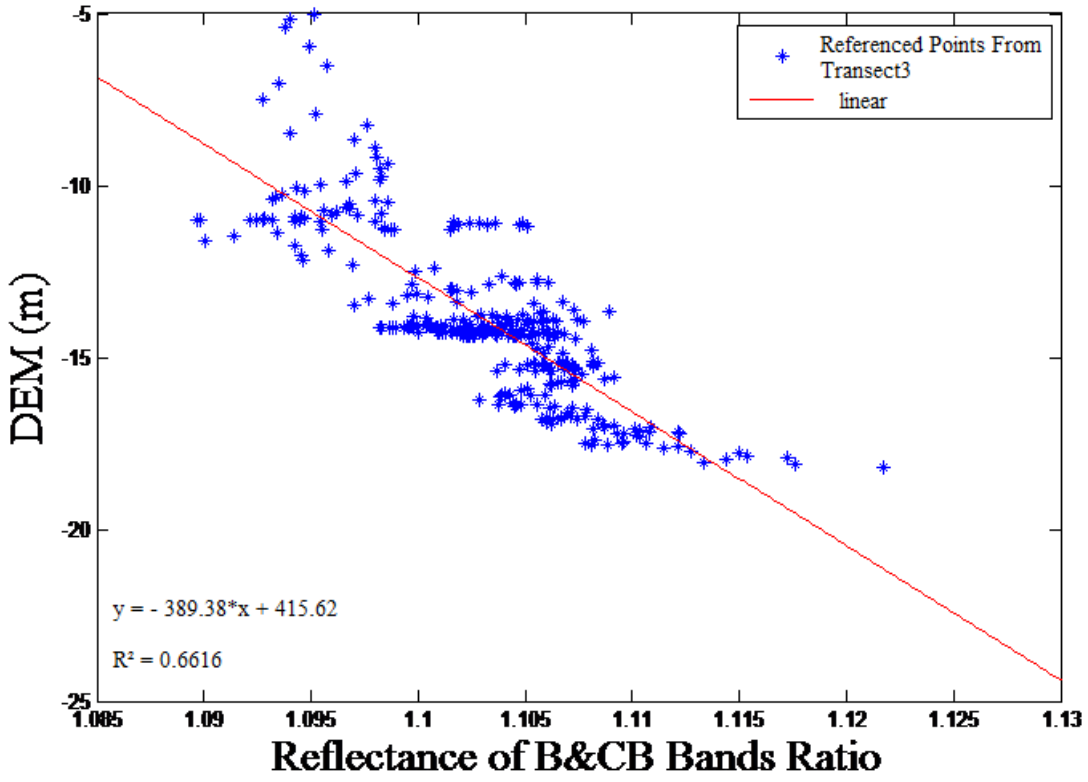

Figure A-9: Linear Regression for Blue/Coastal blue bands along Transect3. The x-axis is the ratio value and y- axis is the corresponding ground truth (DEM) Value at that pixel.

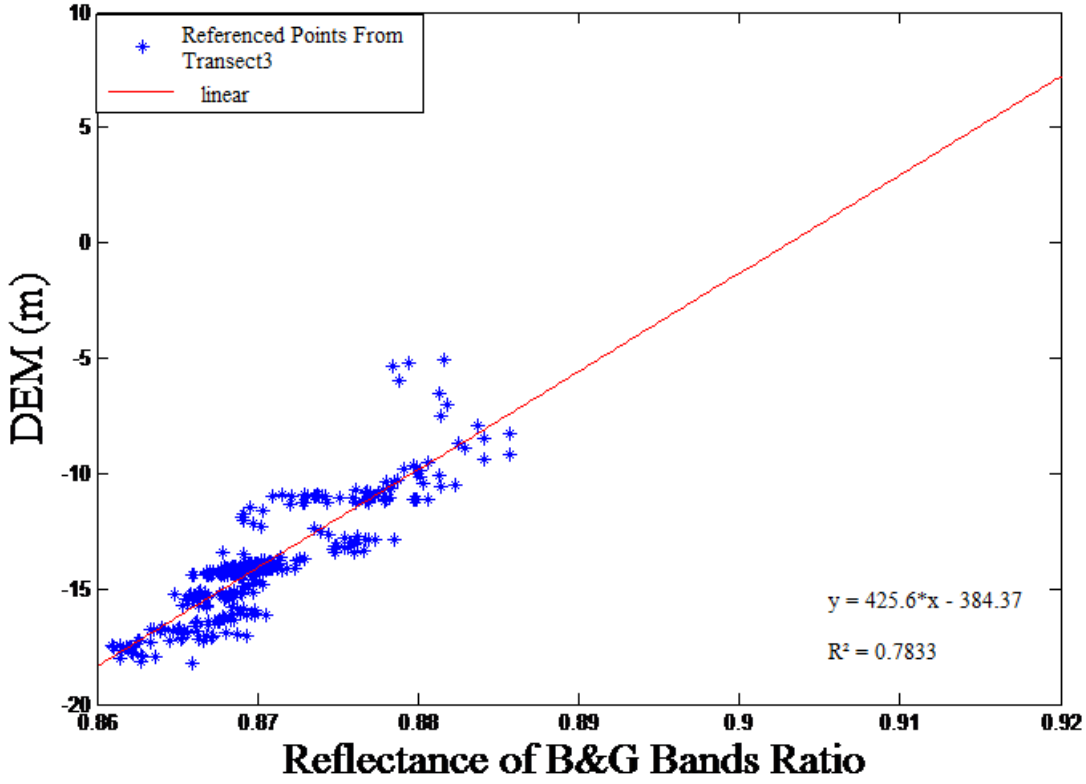

Figure A-10: Linear Regression for Blue/Green bands along Transect3. The x-axis is the ratio value and y- axis is the corresponding ground truth (DEM) Value at that pixel.

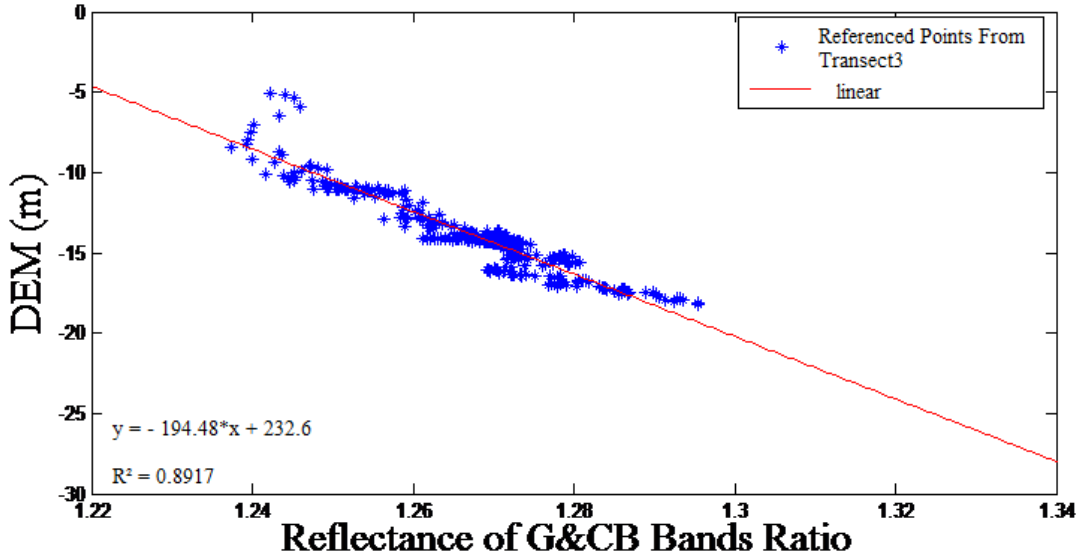

Figure A-11: Linear Regression for Green/Coastal blue bands along Transect3. The x-axis is the ratio value and y- axis is the corresponding ground truth (DEM) Value at that pixel.

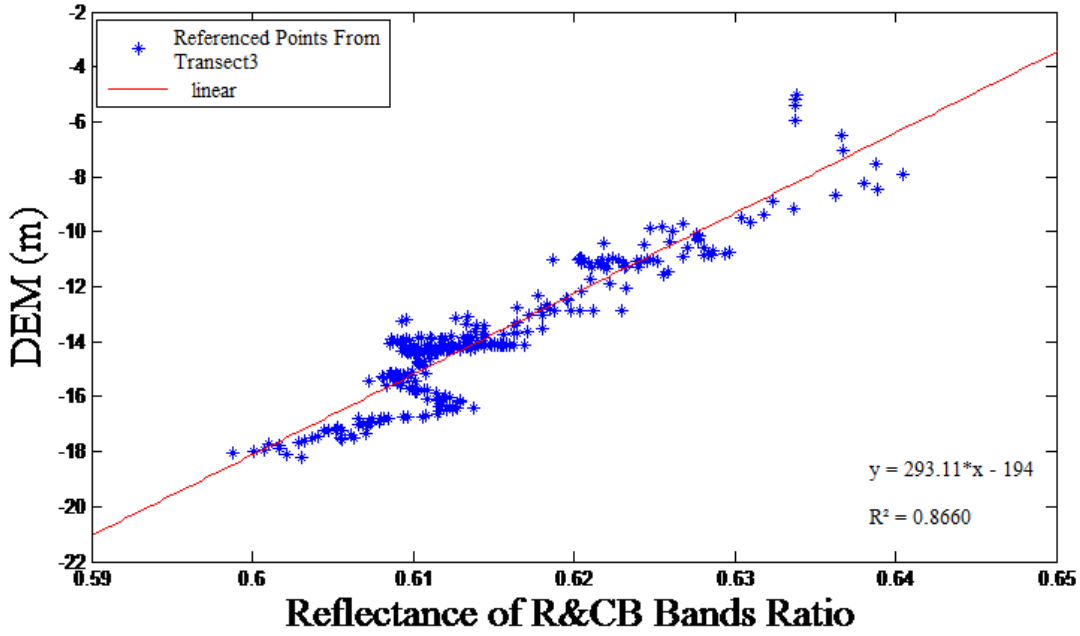

Figure A-12: Linear Regression for Red/Coastal blue bands along Transect3. The x-axis is the ratio value and y- axis is the corresponding ground truth (DEM) Value at that pixel.

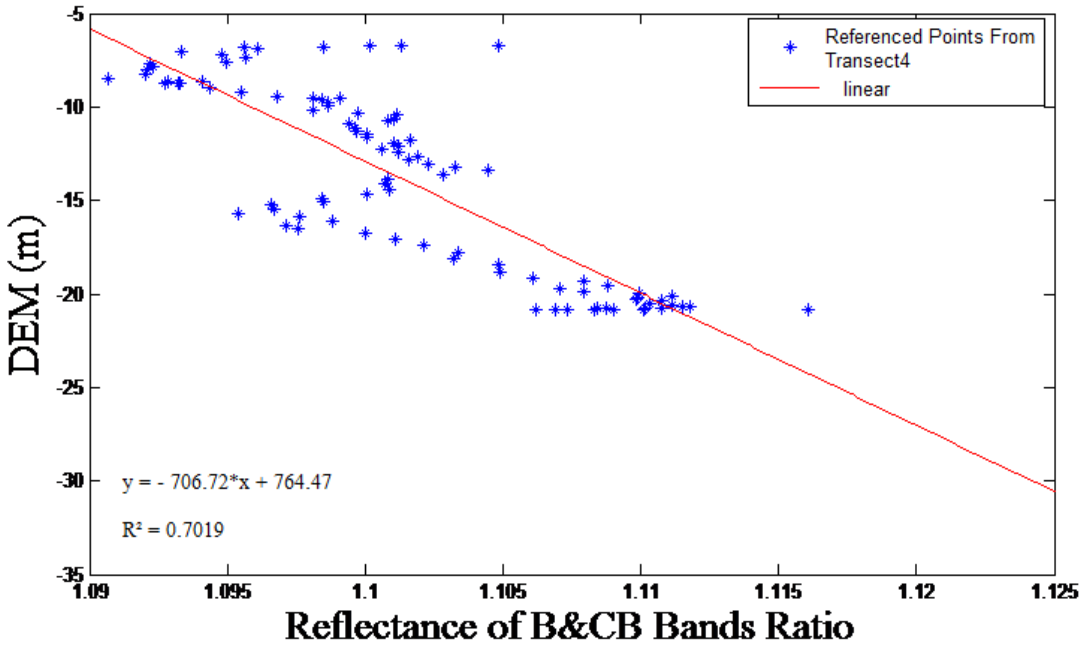

Figure A-13: Linear Regression for Blue/Coastal blue bands along Transect4. The x-axis is the ratio value and y- axis is the corresponding ground truth (DEM) Value at that pixel.

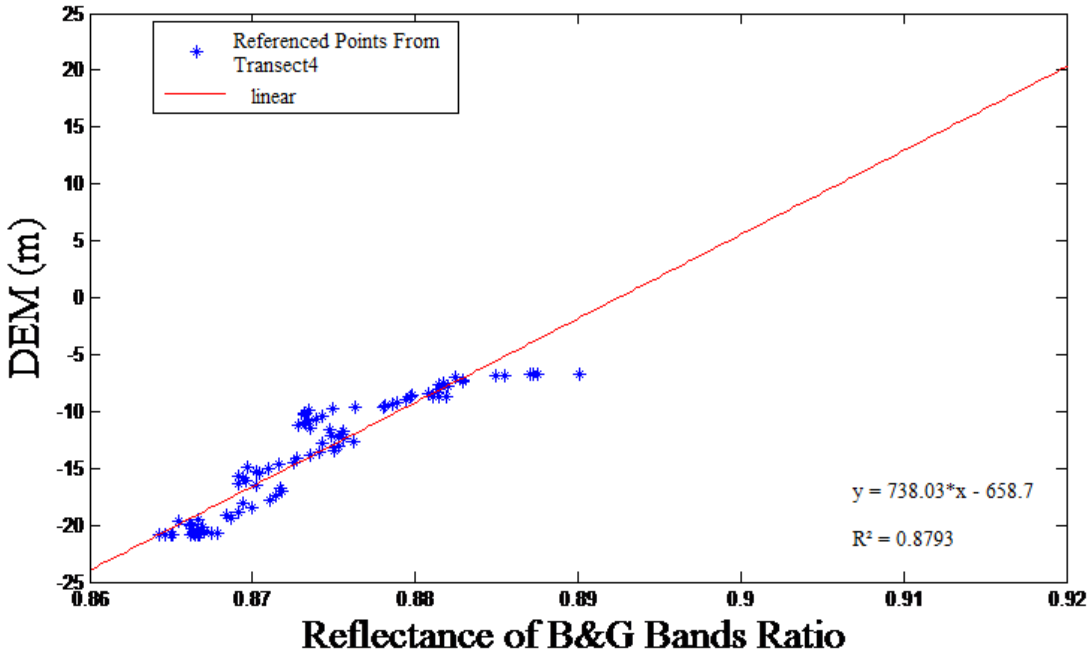

Figure A-14: Linear Regression for Blue/Green bands along Transect4. The x-axis is the ratio value and y- axis is the corresponding ground truth (DEM) Value at that pixel.

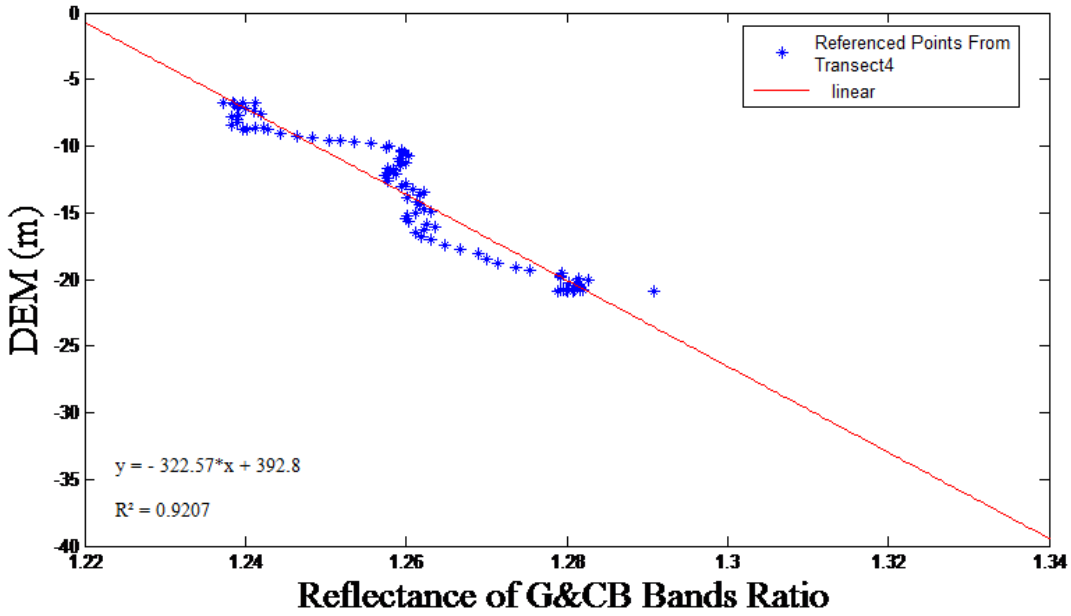

Figure A-15: Linear Regression for Green/Coastal blue bands along Transect4. The x-axis is the ratio value and y- axis is the corresponding ground truth (DEM) Value at that pixel.

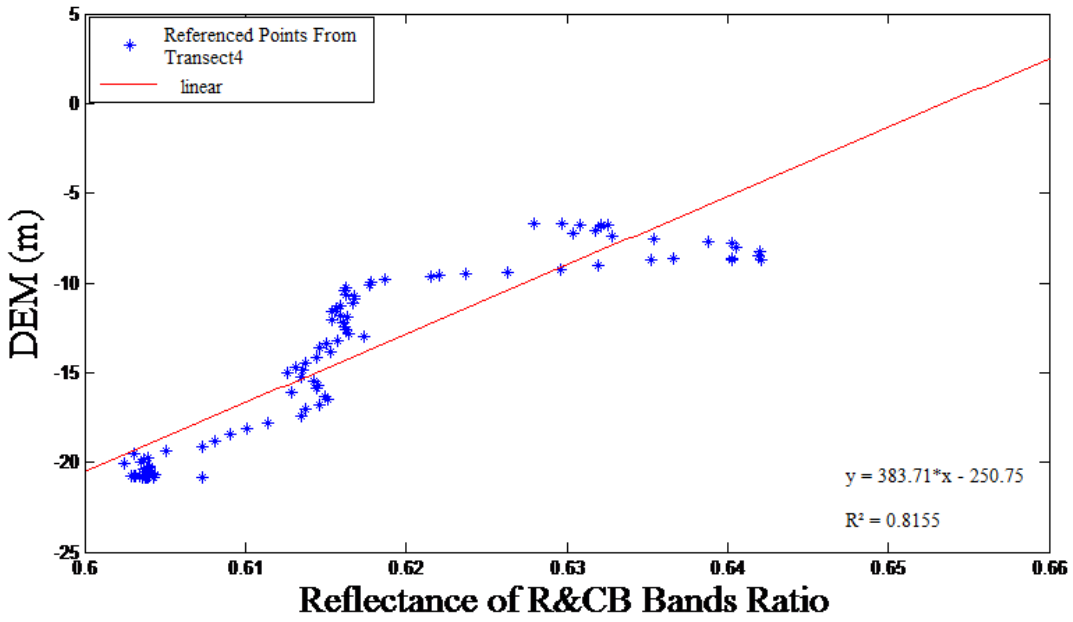

Figure A-16: Linear Regression for Red/Coastal blue bands along Transect4. The x-axis is the ratio value and y- axis is the corresponding ground truth (DEM) Value at that pixel.

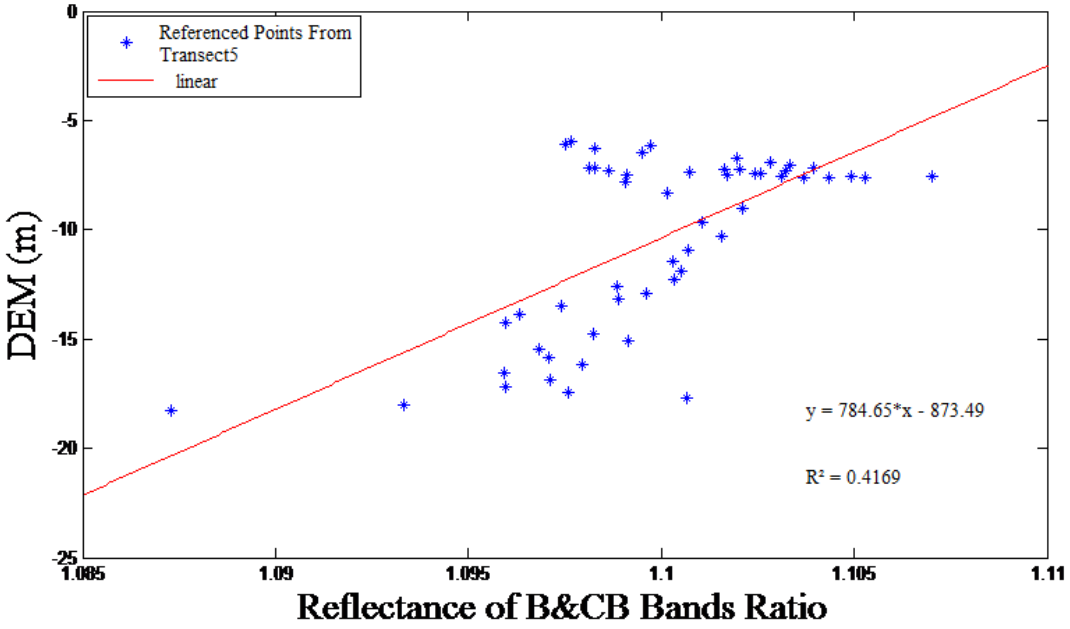

Figure A-17: Linear Regression for Blue/Coastal blue bands along Transect5. The x-axis is the ratio value and y- axis is the corresponding ground truth (DEM) Value at that pixel.

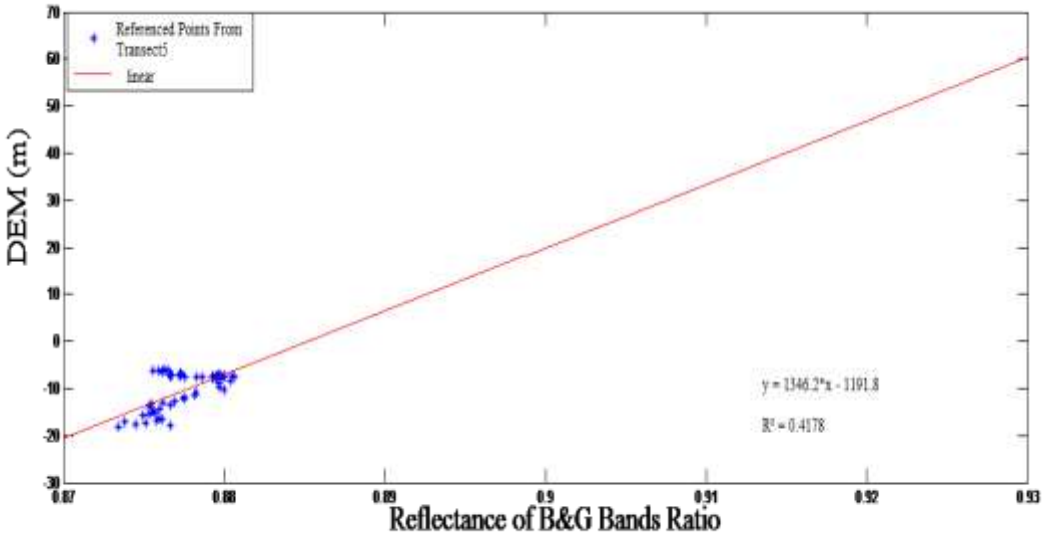

Figure A-18: Linear Regression for Blue/Green bands along Transect5. The x-axis is the ratio value and y- axis is the corresponding ground truth (DEM) Value at that pixel.

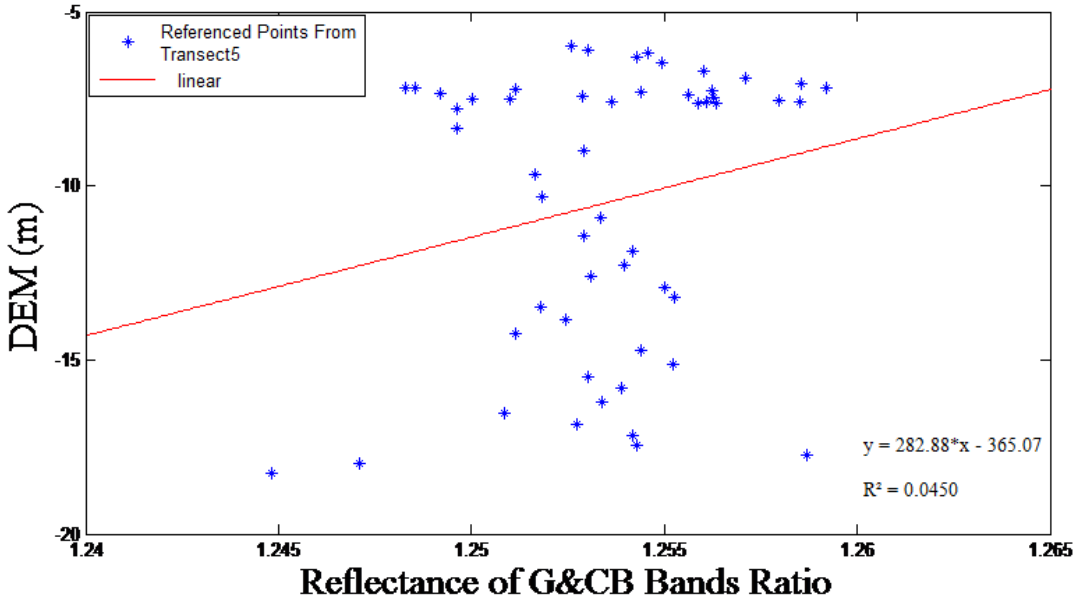

Figure A-19: Linear Regression for Green/Coastal blue bands along Transect5. The x-axis is the ratio value and y- axis is the corresponding ground truth (DEM) Value at that pixel.

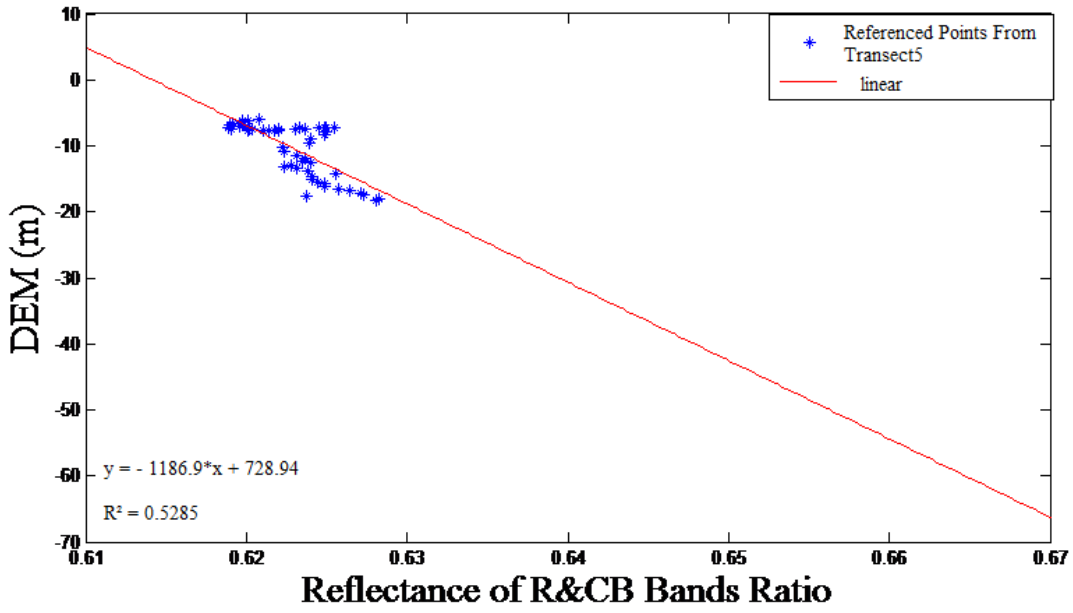

Figure A-20: Linear Regression for Red/Coastal blue bands along Transect5. The x-axis is the ratio value and y- axis is the corresponding ground truth (DEM) Value at that pixel.